A national laboratory of the U.S. Department of Energy
Office of Energy Efficiency & Renewable Energy

National Renewable Energy Laboratory

Innovation for Our Energy Future

Subcontract Report
NREL/SR-520-38679
October 2005

Innovative Approaches to Low-Cost Module Manufacturing of String Ribbon Si PV Modules

Final Subcontract Report
March 2002 – January 2005

J.I. Hanoka
Evergreen Solar
Marlboro, Massachusetts

NREL is operated by Midwest Research Institute • Battelle Contract No. DE-AC36-99-GO10337

Subcontract Report
NREL/SR-520-38679
October 2005

Innovative Approaches to Low-Cost Module Manufacturing of String Ribbon Si PV Modules

Final Subcontract Report
March 2002 – January 2005

J.I. Hanoka
Evergreen Solar
Marlboro, Massachusetts

NREL Technical Monitor: K. Brown
Prepared under Subcontract No. ZDO-2-30628-09

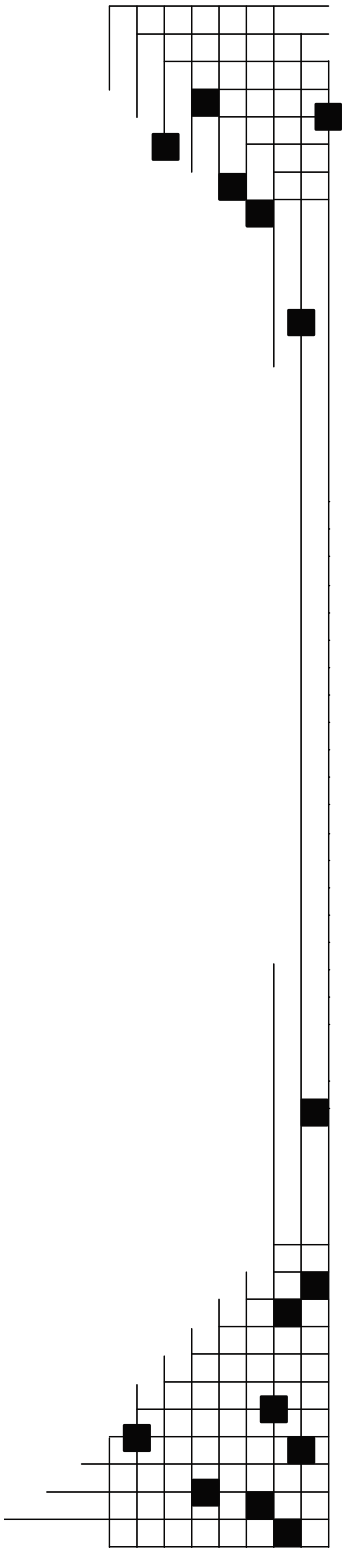

National Renewable Energy Laboratory
1617 Cole Boulevard, Golden, Colorado 80401-3393
303-275-3000 • www.nrel.gov

Operated for the U.S. Department of Energy
Office of Energy Efficiency and Renewable Energy
by Midwest Research Institute • Battelle

Contract No. DE-AC36-99-GO10337

EXECUTIVE SUMMARY

This report summarizes the work done over an approximate three year period, from March, 2002 through January, 2005. The initial project had the following objectives:

- Advances in the Continuous Growth of String Ribbon
- In-line Diagnostics in Ribbon and Cell manufacturing..
- Advances in High-volume, Scalable Cell Making Technology.
- Advances in Monolithic Modules.

As a result of faster than originally anticipated progress made in the first two objectives, the last objective was brought to a close about mid-way through the project, and greater emphasis was placed on the first two objectives.

Advances in the Continuous Growth of String Ribbon

The development of a method to grow dual ribbons from a single crucible (dubbed Gemini) was the most significant accomplishment over this project. This project went through four stages, from initial R&D concept phase to final full production implementation. This development resulted in a number of significant advances in silicon ribbon growth. Among these was a more than doubling of throughput per crystal growth furnace/ per day; improvements in the hot zone design and in-line diagnostics that resulted in yield improvements of 10% in crystal growth, 6% in cell and module making, increases in machine uptime of 12% and an overall reduction in consumables costs by nearly 50%. Net result for Evergreen was a 33% reduction in direct manufacturing costs. This is a very substantial outcome.

In-line Diagnostics in Ribbon and Cell Manufacturing..

In-line diagnostics have been employed to create a more robust, easily reproduced ribbon machine. These improvements have yielded a 2x reduction in the start-up time for new growth machines. Methods for measuring melt temperature accurate to +/- 0.3^{o}C, a means for determining melt depth to +/- 12 microns, and an in-situ thickness measurement technique that is accurate to +/-0.8 microns have all been developed and deployed in production.

Advances in High-volume, Scalable Cell Making Technology.

In-line processing has been developed with particular emphasis on the diffusion and metallization areas. Diffusion has continued with the so-called no-etch process whereby wafers from crystal growth go directly into p-n junction formation with no intervening chemical processing at all. A detailed study and process improvements on controlling the surface oxide layer formed during growth were key to allowing this to succeed. In the metallization area, in-line contact formation has been extensively developed and deployed in production.

Advances in Monolithic Modules.

Although this part of the overall project was not consummated with entry into production, an important aspect of the overall technology was shown. A combined system of a conductive adhesive and Evergreen's proprietary backskin material was demonstrated to show excellent long term reliability for monolithic modules that contain cells with wrap-around contacts. This solves one of the major problems in finding a low-cost, elegant method for making a monolithic module.

The combined success of the first three objectives has resulted in Evergreen expanding to full capacity in its Marlboro, MA plant to 15 MW/yr with the lowest direct manufacturing costs it has ever achieved.

TABLE OF CONTENTS

TABLE OF CONTENTS

LIST OF FIGURES

LIST OF FIGURES (con't)

Figure # **Description** **Page #**

Advances in the Continuous Growth of String Ribbon

Development of a multiple ribbon growth system. (Project Gemini)

Evergreen's String Ribbon method as practiced for a single ribbon from a crucible is shown In Figure 1a. Two high temperature string materials are used to stabilize the edges of a ribbon grown vertically directly from the melt. The silicon melt is contained in a graphite crucible and the ambient gas is argon. The basic process is robust and virtually continuous. String Ribbon machines are run in production on a 24/7 basis. The feedstock material consists of small, spherical shaped particles of silicon on the order of 1mm in diameter and are formed in a fluidized bed that utilizes the thermal decomposition of high purity silane. Such a feedstock morphology lends itself to continuous, controlled feeding and has been a factor in making String Ribbon a virtually continuous process. In addition to the obvious benefit of not having to saw and lose about half the silicon, the String Ribbon method of growth directly from the melt also allows for control of the as-grown ribbon surface so that no etching of any kind is needed prior to cell making. The as grown ribbon has a smooth and highly reflective surface.

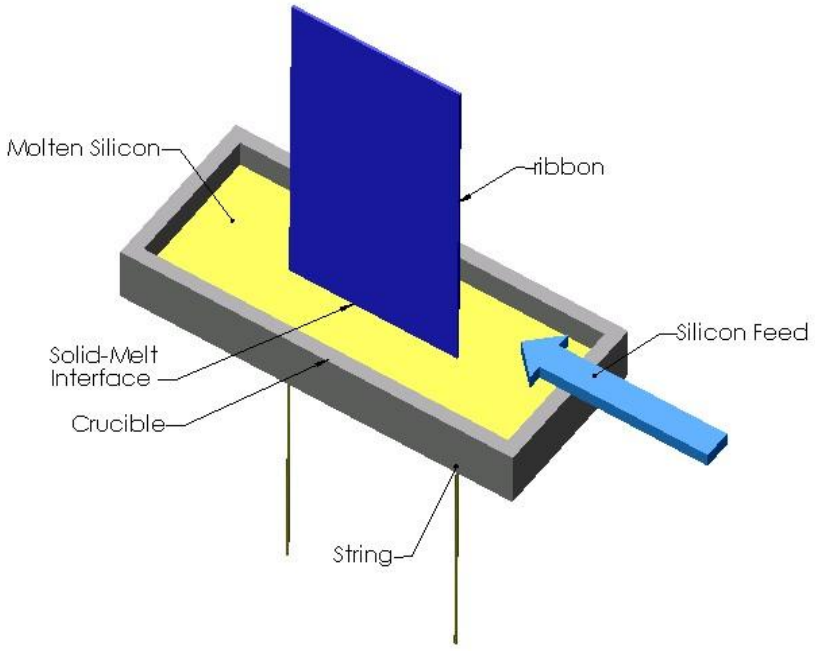

Figure 1a – Single ribbon growth

In order to further reduce costs, a method for multiple ribbon growth from a single crucible was developed. This project resulted in the growth of dual ribbons from a single crucible and was termed "Gemini". Over the course of this PVMR&D project, Gemini began first as an R&D concept and then into a pilot phase, and finally into full production. In Gemini, shown in Figure 1b, two ribbons are grown, back-to-back, out of a single crucible.

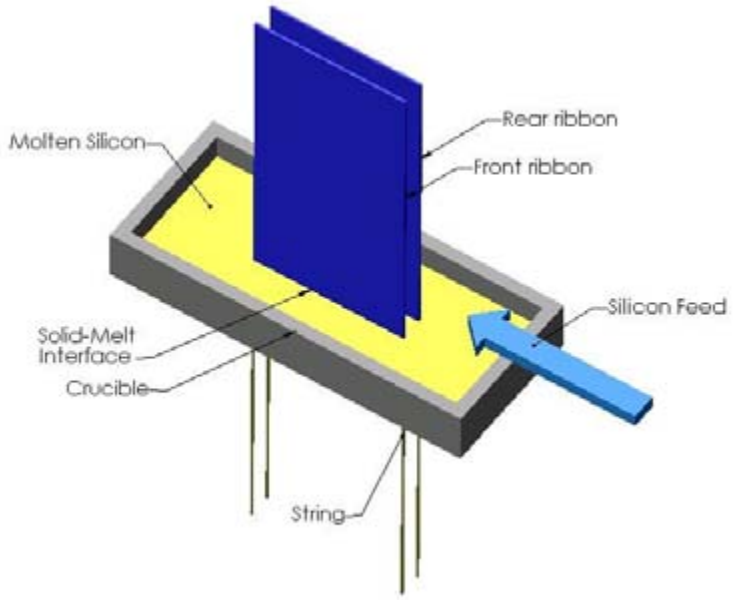

Figure 1b - Dual ribbon (Gemini) in the String Ribbon process.

It can be seen that four strings are involved instead of two as needed for single ribbon growth. Thus, with most everything being equal except principally silicon costs, nearly twice as much ribbon is obtained from a single crucible and furnace for virtually the same consumable, labor, and capital costs. The material, as now grown, is 300 microns thick, 8 cm. wide and it is grown into 2m long strips that are then removed from the growth machine without interrupting growth. These strips are then cut with a laser into 15 cm long solar cell blanks. The ribbon is B doped to 2-3 ohm-cm. Figure 2 shows the upper portion of a Gemini machine in operation where it can be seen that two ribbons are growing.

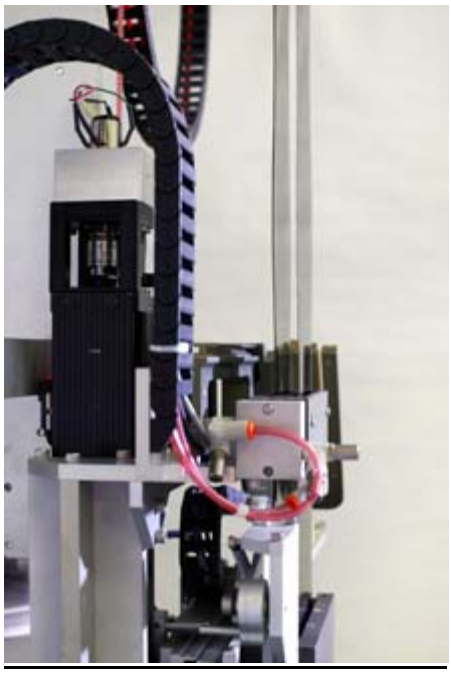

Figure 2 - Dual Gemini ribbons growing.

The Gemini project was conducted in four phases, listed below. Each of these will be discussed separately.

- **Phase A - fundamental issues addressed in R&D .**
- **Phase B - pilot line.**
- **Phase C - in-line diagnostics, controls and instrumentation in pilot.**
- **Phase D - full production at a 15 MW/yr rate.**

Phase A - fundamental issues addressed in R&D.

Several technical hurdles had to be overcome in the R&D phase before Gemini could be considered for pilot production. These included:

- (a) insuring that the molten silicon menisci surrounding each of the two Gemini ribbons did not interfere with each other.
- (b) correcting for the expected difference in the radiative environment surrounding each ribbon,
- (c) developing robust mechanical means for harvesting two ribbons from a growth machine, and
- (d) suitable in-line diagnostics for such things as melt depth, ribbon thickness, and crucible temperature.

Silicon menisci - The problem that had to be solved here can be visualized from the following considerations: molten silicon wets the sides of a graphite crucible and also forms an angle of about 11^{o} with the growing ribbon. The result is that in a cross-sectional view of the molten silicon in the crucible, looking parallel to the ribbon edge, it will show a flattened "U" shape as seen in Figure 3.

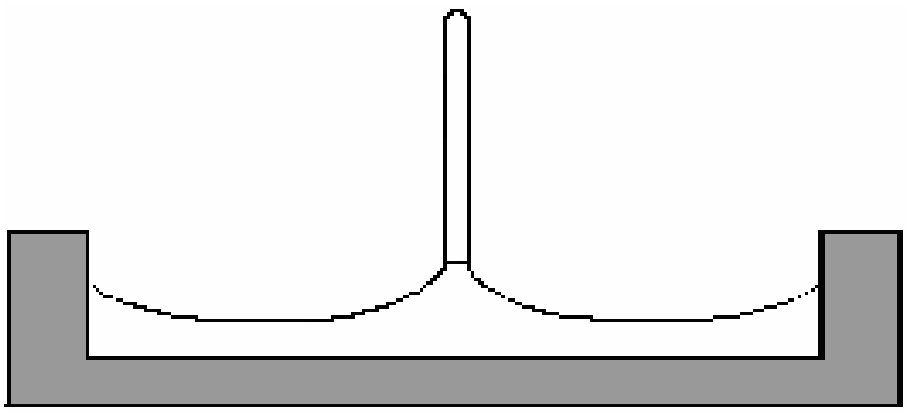

Figure 3 – Illustrating a meniscus shape for a single ribbon in a crucible. Shown is a cross section through a crucible where the ribbon is seen end on.

Similarly, if there were two ribbons growing near each other as in the Gemini configuration, there would be a U shaped molten silicon pattern between them as well. The ribbons as they grow are only pinned at their ends by the string material with the consequence that the ribbon centers can move. The driving force to reduce surface energy will result in the two ribbons trying to merge into each other at their centers. If this were to occur, the result would look, from the top, like an X with curved sides.
Another way to say this is that the highly curved meniscus between the two ribbons, can, in order to reduce surface energy, force the two Gemini ribbons together. Such an event obviously prevents the growth of two discrete ribbons.
An important development in the early Gemini work was a method to avoid this problem and control the shape of the meniscus surrounding each of the two ribbons in a Gemini configuration.

Radiative environment - One would naturally expect that the radiative environment surrounding the two Gemini ribbons to be different and to show an asymmetry that could then affect the growing ribbon. Such an asymmetry would be expected to result from the geometric asymmetry present in the Gemini configuration. In this case, this problem was also successfully addressed by modification of the afterheater in the hot zone so that any possible thermal asymmetry in the radiative environment surrounding each ribbon could be minimized. This was achieved through the use of materials with the appropriate thermal conductivity and emissivity. There is still a finite asymmetry in the overall ambient gas flow for the inside and outside surfaces of the Gemini ribbon. This is still manageable from the point of view of the thin oxide layer that forms on the ribbon surface and is discussed further in the section on the no-etch process discussed in the solar cell portion of the report.

Thermal Profiles - This was undertaken in order to explore some basic issues of the effects of measurement position, time, thermal regulator position, and gas flows on the thermal profiles in the afterheaters and in particular how this might affect growth at the edges of the ribbon. The idea here was to find ways to form thicker edges, as thin edges contributed, in this initial work, to lower yields.

The afterheater used for this initial work was an earlier version of the overall redesigned hot zone – the so-called “Gemini II”. These issues are expected to have similar effects on newer afterheater configurations, and thus can inform our thinking on any future design direction.

Thermal profiles were generated by hanging an unshielded thermocouple down from the furnace top over a crucible with silicon melt in a complete hot zone, but without any ribbons present. The ribbons are a very important element in the thermal performance of the after- heaters, by conducting heat up from the melt, radiating to and blocking radiation from the after heater elements, and engaging and directing gas flows.

Thus the profiles do not show the ribbon temperature, but are only a representation of the thermal environment within which the ribbon cools. However, since the ribbons are thin, with high surface area and low thermal mass, their temperature profiles are expected to be similar to their environment except in areas of very high gradient.

Measurement Position - The first three profiles measured temperatures in the plane of the back ribbon, midway between the ribbons, and in the plane of the front ribbon, respectively, under nominally identical furnace conditions (thermal regulator position, gas flows, set point temperature). Subsequent profiles indicated that within the accuracy of this measurement, there is no difference between the front and back ribbon positions.

Lateral Profile results - All the thermal profiles show that at meniscus height the temperature seen by the thermocouple is hotter at the ribbon edges than at the ribbon center. However, the edges cool faster than the center, so that the edges of the ribbon are cooler than the center of the ribbon at a height of several cm. above the meniscus height.

Cooling the ribbon in a “frowning” profile, with the edges colder than the center, works well for reducing stress and is used in other crystal growth systems. Figure 4 shows a typical profile.

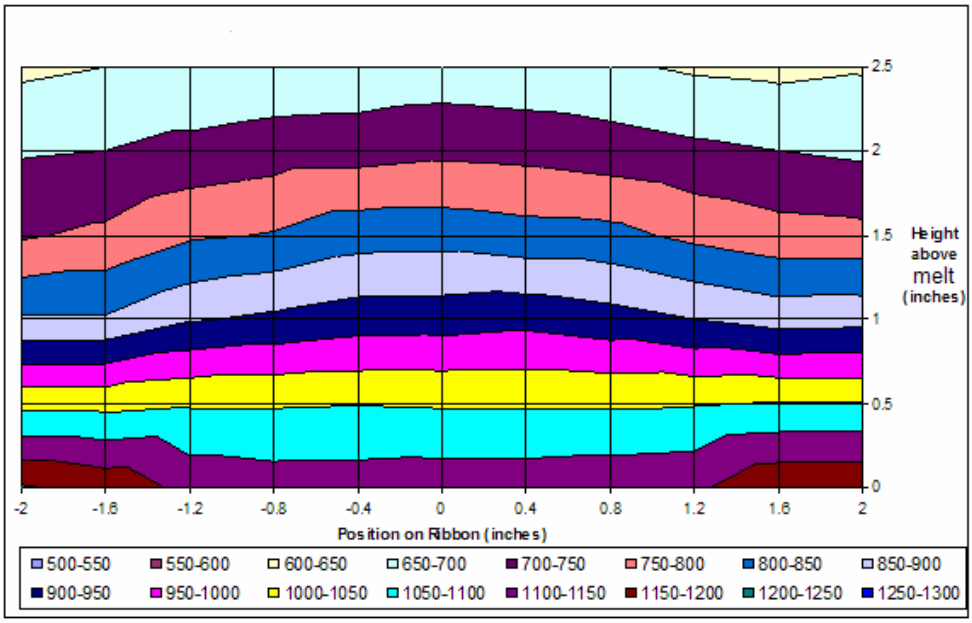

Figure 4 -Typical lateral thermal profile.

Gas Flow Effects – Not surprisingly, there were significant gas flow effects that changed the thermal environment. Comparison profiles were taken using the present gas flows and with the ambient gas turned off so that natural convection would be operative. The temperature increased on the order of 50°C throughout the profile, and the fluctuation in temperature at each point increased from about +/- 5°C to roughly +/- 20°C, showing increased natural convection. Figure 5, shows how small changes in the ambient gas flow can also result in significant changes in the thermal distribution. The vertical scale is height above the melt in inches, the horizontal scale is the position along the ribbon and the colors represent different temperature ranges, in 10 degree increment.

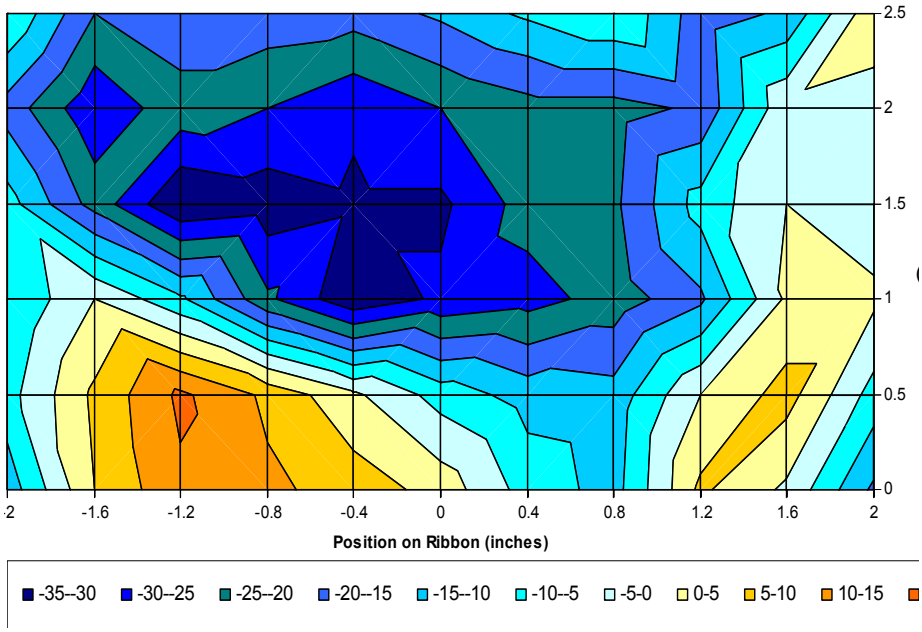

Figure 5 – Gas flow effects

However, in a later parameter sensitivity study, it was found that the argon ambient gas flow setting could be changed by +/- 50% without any adverse effects on the yield or machine uptime of the growing ribbon. This indicated that the parameter space for these settings for gas flow is quite broad. It also highlighted that the lab determinations of thermal profile effects while useful, were not a substitute for empirical results.

Vertical Profile results - Incorporated into the overall hot zone design are devices that allow for thermal regulation at various points along the crucible. Figure 6 shows vertical profiles as a function of positions of these thermal regulators. The upper profile is with the regulators in the uppermost position and the lower profile is for the regulators in the lowermost position. This type of data was useful in charting the

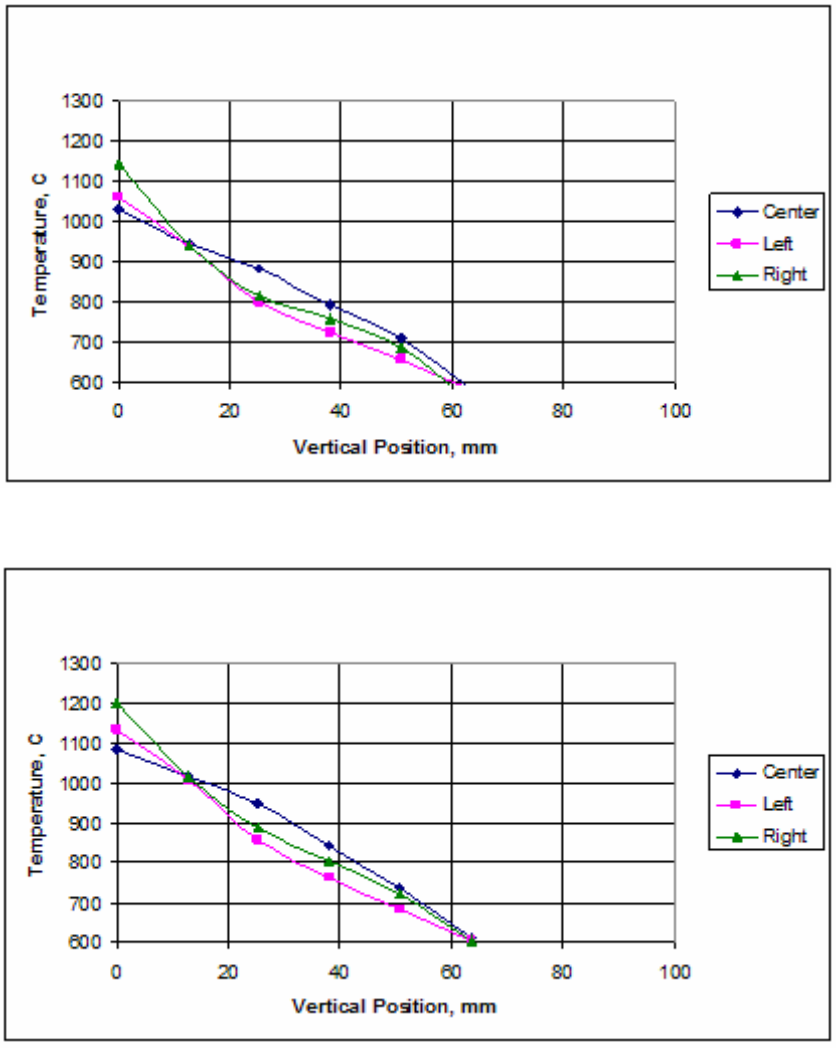

Figure 6– Vertical thermal profiles for various settings of the thermal regulators. Upper graph – thermal regulators in highest position. Lower graph – thermal regulators in lowest position.

Parameter space for these particular thermal regulators. The figure below ,Figure 7, shows the high sensitivity of the hot zone to small design changes. In this case the afterheater was moved only 0.1 “and the thermal profile changed significantly. The vertical scale is height above the melt in inches, the

horizontal scale is the position along the ribbon and the colors represent different temperature ranges, in 10 degree increments.

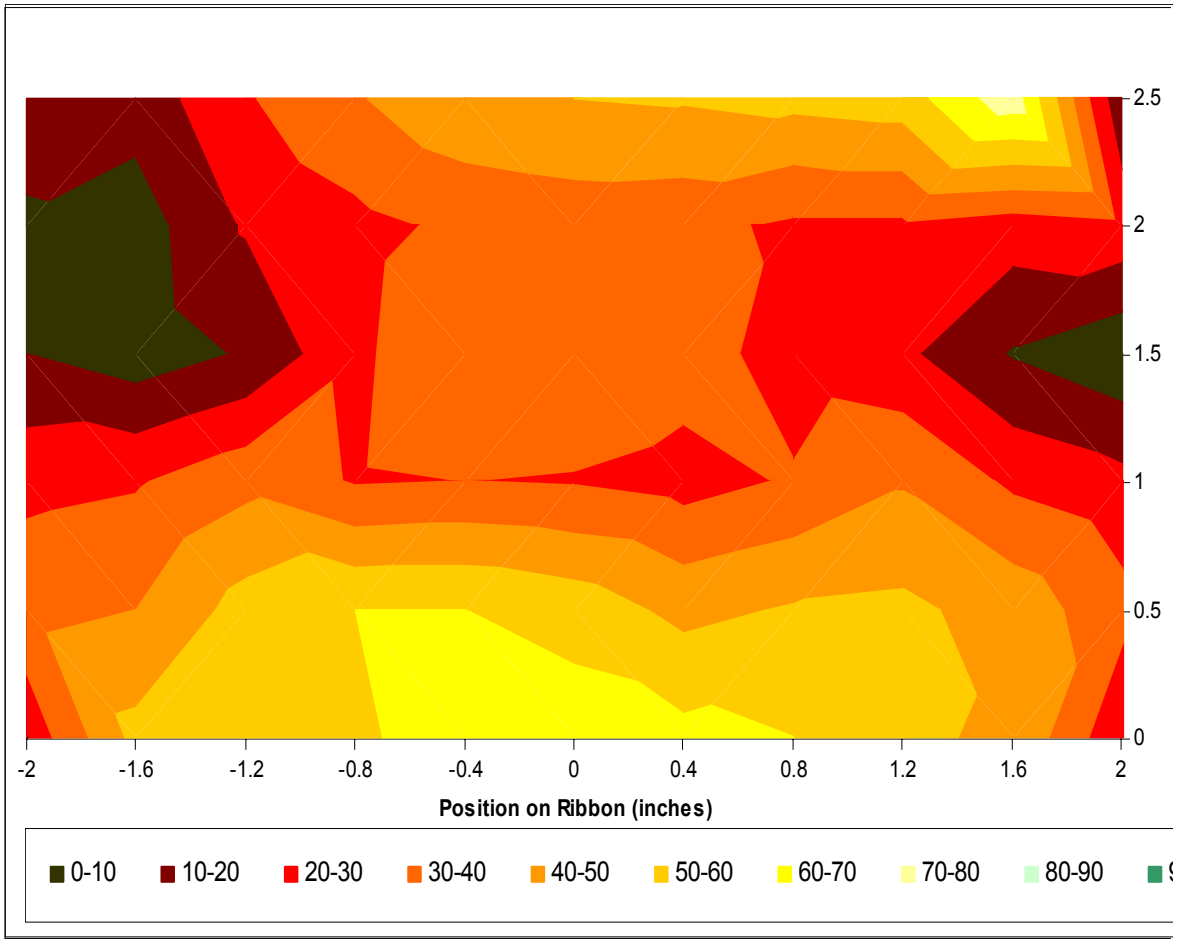

Figure 7 - Illustrating the sensitivity of the hot zone thermal distribution to small geometric changes.

An effort was made at using finite element modeling to study gas flow effects. Some initial work started with ignoring thermal effects and looking at possible flow patterns by introducing different gas flow assumptions. An example is shown in Figure 8, but it was not clear in the end just how useful the modeling work could be. Again, empirical iteration proved to be more useful.

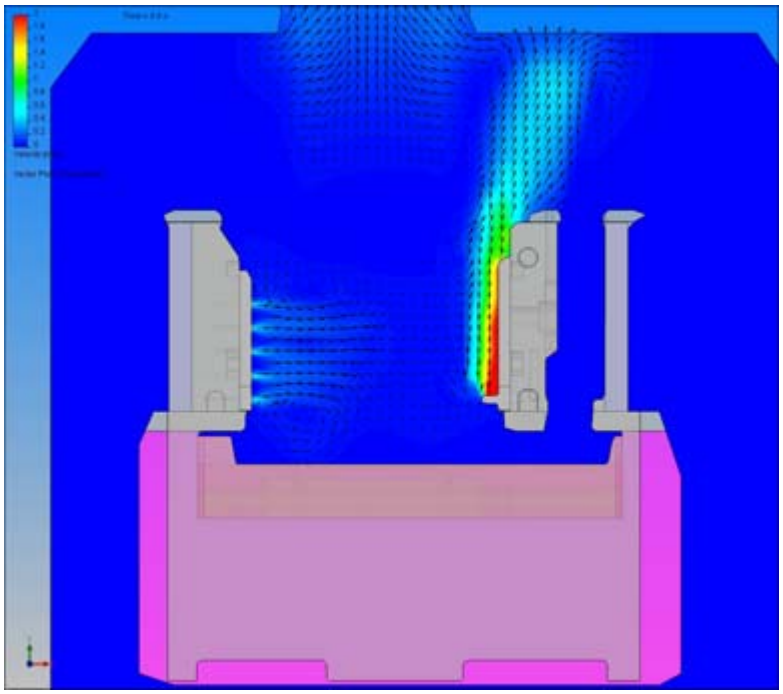

Figure 8- Finite element modeling.

In general, some of the sensitivities discussed above highlighted the need to design a hot zone that exhibited a maximum of robustness in regard to some of these parameters. A number of empirical iterations, as well as very significant improvements in controls and instrumentation finally resulted in a production ready hot zone, as will be described in further sections in this report.

The final hot zone design (discussed in the next two sections) was found to be quite robust and very amenable to of scaling. Figure 9 below shows the inventor of Gemini and the designer of the hot zone, Rick Wallace, holding a Gemini strip.

Figure 9 - Rick Wallace, the inventor of the Gemini method.

Phase B - pilot line.

As soon as the concept and feasibility work was completed in the lab, a team was set up that included the R&D personnel, engineering people, and production people. Meetings were scheduled on a weekly basis and communication between all groups was fostered very intensively.

Harvesting Gemini Strips -Concurrent engineering principles were applied almost at the outset to address what was believed to be a possible major engineering issue, that of simultaneously harvesting two ribbon strips. After a 2 m long strip of ribbon has grown in a single ribbon configuration, it is diamond scribed at the top of the furnace and gently snapped to disconnect it from the ribbon still growing.

Having two ribbons present in the Gemini configuration presented some mechanical problems with the procedure and apparatus used for single ribbon machines. For Gemini, following the scribing operation, it would now be necessary to remove both ribbons at the same time. This required that these ribbons be firmly gripped at their tops and also that this grip would release simultaneously for both ribbons. This called for some careful mechanical design work on the part of Evergreen's engineering team.

In the course of solving this problem, the ultimate design turned out to be an improvement on the original design used for the single ribbon machines. The net result has been that the production operators have found the new Gemini system even easier to use than the older, single ribbon system. At present, a production operator can harvest two ribbons from a Gemini furnace quite easily and this is shown in a photograph in Figure 10.

Figure 10 - Production operator removing two Gemini ribbon strips simultaneously.

As Gemini progressed into the pilot phase, several iterations of the hot zone were tested almost simultaneously. Early experience at Evergreen had shown that results obtained on short runs in the lab do not necessarily translate into successful production results. That is, it was necessary to run a process for weeks at a time under 24/7 conditions before clear conclusions on the efficacy of this particular

process can be demonstrated with any assurance. Hence the pilot phase was done in the production area with 10 Gemini machines devoted to it.

Key requirements for a production worthy hot zone and process:

- Flat ribbon
- High yields and high machine uptime
- Ribbon surface free of surface layers
- Reduced part count
- Long run lengths.

While the genesis of the work concerned with the above requirements was in Phase 1 in the R&D lab, the bulk of the results were obtained in Phase 2, the pilot phase. As will be shown further on in this report, the final hot zone chosen satisfied these criteria quite well.

Flat ribbon - Evergeen's prior experience in hot zone design and in engineering of crystal growth furnaces was utilized fully to address the ribbon flatness issue. With improvements in the overall hot zone design as well as the controls and instrumentation advances described further on, it was found that extremely flat ribbon could be grown in the Gemini process when using the redesigned hot zone.

In fact, the ribbon was so flat now that the robots used to pick up the ribbon blanks to align them for the diffusion process had to be modified to avoid the stacked wafers from sticking to each other. This enhanced flatness had significant yield benefits downstream as will be discussed further. A stack of 18 Gemini strips is shown on the right in Figure 11.

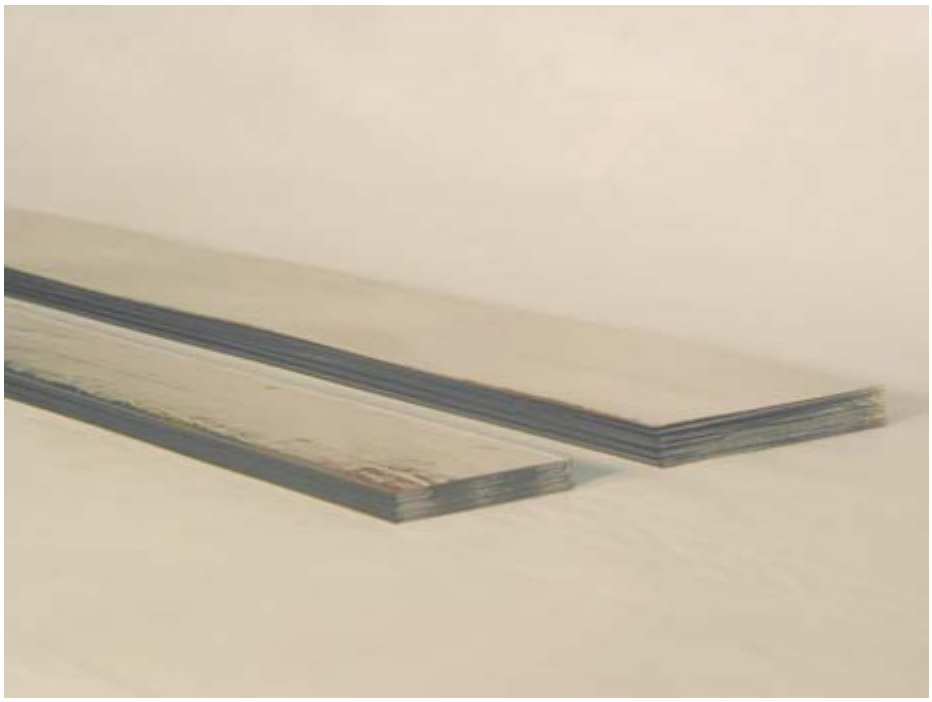

Figure 11 – On the right is a stack of 18 flat Gemini strips. (The stack on the left is an experimental one, not related to Gemini)

High yields and high machine uptime

During the pilot phase, a number of items that could affect yield and machine uptime were identified. These included thin edges, thickness variations in the ribbon, inadequate thermal control at the growth interface and in the section of the crucible where the feedstock was introduced. Where warranted and possible, improvements were designed, developed, and then tested on the pilot line. Thickness variations and thermal control are dealt with in the later section termed “In-line diagnostics” even though they were developed and debugged during the pilot phase.

Thin ribbon edges

One earlier issue with even higher production yields was that of thin ribbon edges. A detailed investigation of this effect and means to ameliorate it was undertaken. Two areas in particular were studied. One was that of possible changes in the Coefficient of Thermal Expansion (CTE) values of the string material and the other involved a detailed study of the thermal profile across the ribbon width. In the case of the latter, the above descriptions of the thermal profile work were examples of this being studied in the R & D lab.

Choice of a string material was dictated by these requirements:

- non-metallic components
- components able to withstand temperatures > 1400^{o}C
- close CTE match with silicon throughout the temperature range

The last requirement was the one that was of greatest concern. When the thin edge problem occurred, there was a concern that the CTE of the string material may have varied due to some variation in the manufacturing process.

Elongation measurements that would allow for CTE determinations of the string material were done. This is a difficult measurement as it must be made at rather high temperatures. Figure 12 shows some typical measurements done up to 1400^{o}C. Recall that the melting temperature of silicon is 1412^{o}C and that silicon is not very plastic below about 1000^{o}C. In Figure 12 the upper curves represent the cooling curve and the lower curves are for the heating curve. These curves indicate that there may be a hysteresis effect. These curves also indicated a possible difference between two batches of string material. One batch did not result in significant edge breakout or thin edges and the other batch did. However, there was no clear signal on this with subsequent determinations.

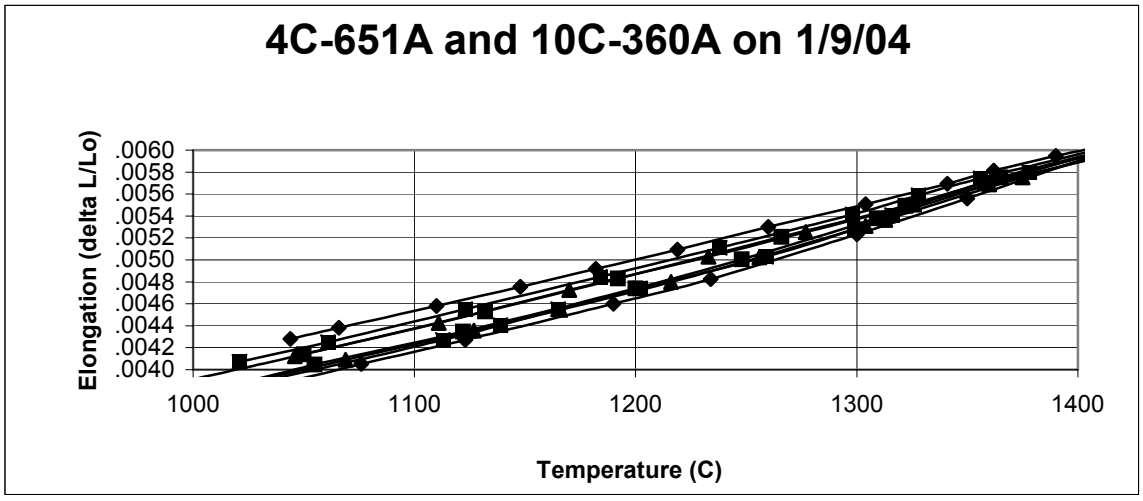

Figure 12 - Elongation measurements of string material.

Machine uptime

This was an extremely important production metric. It is a measure of the actual time that a machine is producing usable ribbon. The factors that determine it are:

- the time to change hot zones when the crucible has eroded
- the time to seed
- the time to reach a steady state once a furnace has been turned on for growth.

With the final hot zone design chosen with its reduced part number and simplified, modular construction the time to change hot zones was reduced by a factor of 3. The introduction of the controls and instrumentation described further on allowed for a shortening of the time to reach steady state by a factor of 2.5. Seeding time was not significantly reduced, but the new design plus some of the in-line diagnostics developed made the overall seeding process simpler and less subjective.

Ribbon surface free of surface layers

Surface layers that can form on String Ribbon are of four general types: SiC, SiO, SiO_2, or a combination oxycarbide of some sort. There are ample quantities of carbon in the form of graphite present in the zone. SiO is invariably formed as there is always a finite amount of oxygen present and SiO is a very volatile material at these high temperatures. SiC can then result from the presence at high temperatures of SiO and some kind of carbon-oxygen volatile species, probably CO or CO_2.

Generally, such surface layers will adversely affect the fill factor of the finished solar cell. Figure 13 below shows the variation in oxide layer thickness that was seen with an earlier Gemini hot zone design (called Gemini 1) As will be shown further, this degree of variation precluded the use of the no-etch process.

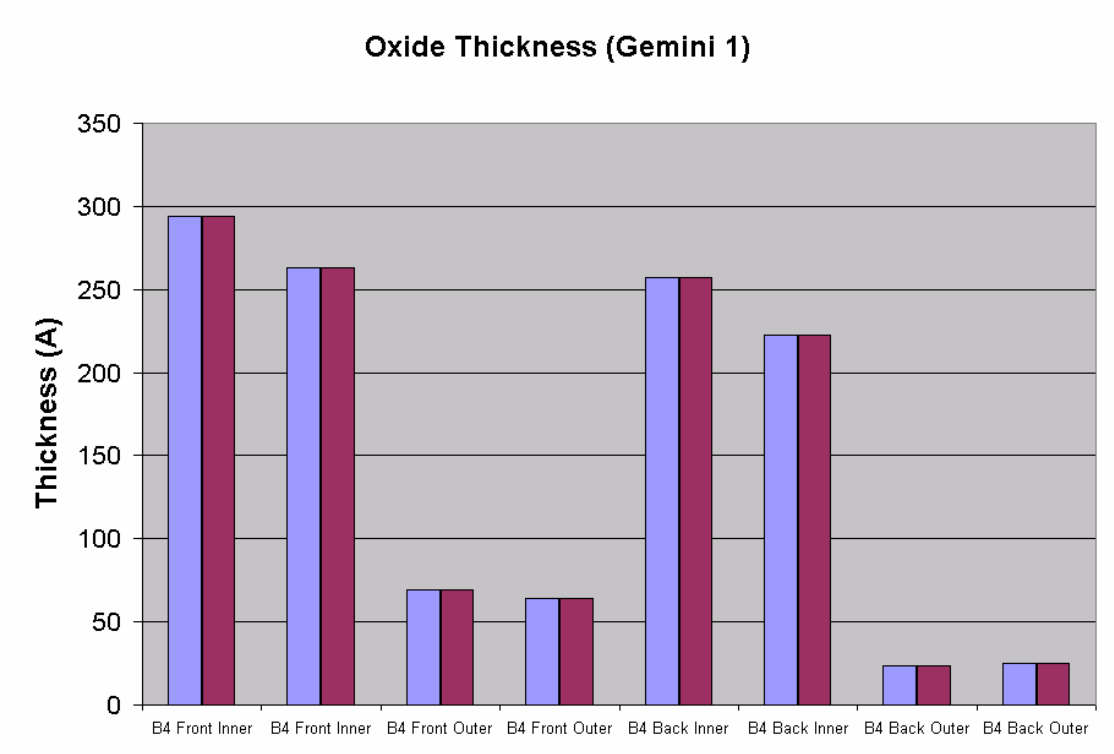

Figure 13 – Oxide thickness variation for both surfaces of two Gemini ribbons.

As a consequence, considerable effort was devoted to modifying the growth environment so that these layers do not form to any degree that is detrimental to solar cell efficiency. They key here was in developing some understanding of the high temperature chemistry surrounding the hot zone and then developing methods to obtain reproducible and usable ribbon surfaces.

It was found that a finite layer of SiO_2 could not be avoided, so it was decided to learn how to control such a layer and then utilize it for the so-called no-etch process described further on in the solar cell section. In that section it will be seen that this effort was quite successful.

Reduced part count

Several design criteria were used in the redesign of the Gemini hot zone. These were: ease of installation of all the parts, ease of alignment, reduced and simplified number of parts. This part of the overall project was extremely successful. The number of parts was reduced by 46%, almost a factor of two, over that of earlier hot zone designs. Furthermore, the final design represented a far more modular approach that avoided possible positioning errors inherent in some of the earlier designs. In addition to lowering the overall cost of the hot zone, this part reduction produced a far simpler structure that was much easier to assemble and this, in turn, reduced the time required to set up a machine.

Long run lengths.

With the redesign of the hot zone, a vastly improved capability in temperature measurement was also introduced (discussed further in the section on in-line diagnostics). Run length is defined as the time that a graphite crucible can be used before it is seriously eroded by the molten silicon. Increased run lengths translates directly into reduced consumable costs. One important result of this enhanced capability in temperature measurement and control, coupled with some thermal design changes allowed for the longest run lengths ever seen for String Ribbon.

Another very important aspect of the pilot phase was the introduction of in-line diagnostic techniques to produce a more uniform ribbon and a more automated system overall. While there remains work to be done for further automation, the diagnostic techniques described in the next section here will provide an excellent foundation for this.

Phase C - in-line diagnostics, controls and instrumentation in pilot.

Thickness control

One of the key aspects of making the Gemini II system provide higher yields, both in crystal growth and in downstream processing is that of thickness control, and this then devolves on the accuracy and control possible with the thickness measurement method. The goal here was an in-situ thickness measuring device with an accuracy of >5x than for the earlier such devices. As an in-line diagnostic tool, this would provide for more uniform ribbon.

The target thickness is 12 mils, 300 microns. The following figure 14 shows a typical thickness scan measured manually across the 8 cm (3.2 “) width of the ribbon. This figure displays several typical features. The central portion of the Gemini ribbon is quite close to the targeted value, with the standard deviation at a very acceptable level. The ribbon tends to thicken closer to the edges and does this somewhat asymmetrically. Finally, at the very edge, the thickness approaches that of the strings.

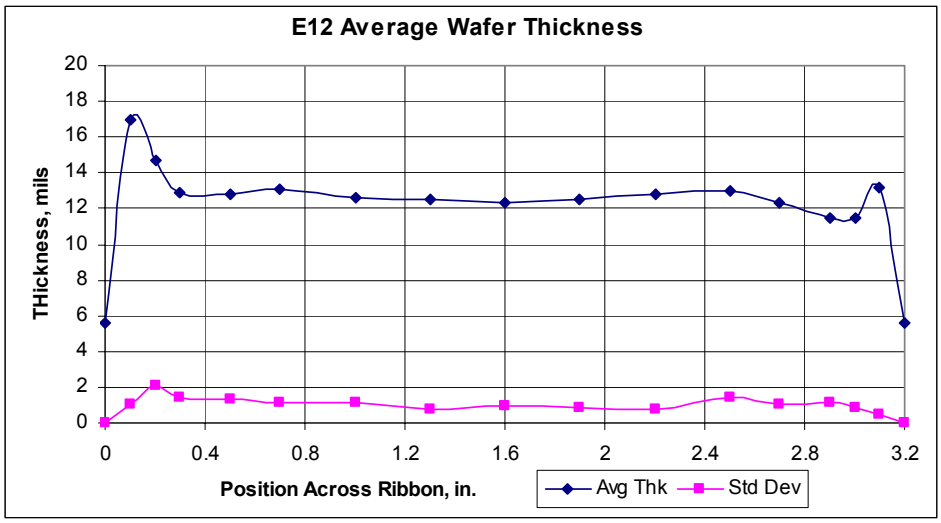

Figure 14– Manually measured thickness across a typical Gemini II wafer.

Previous thickness measuring devices had an accuracy of +/- 1 mil; partially due to temperature variations within the calibration standard, and the use of two calibration standards (one for high, and one for low thickness). The new system uses a much more thermally grounded calibrator, and is based on a more theoretical analysis of the method and the response of its components. In this method, a single known calibration thickness is used along with the known reflection behavior of silicon.

The new thickness device is accurate to within at least +/- 0.3 mils. So this is, at a minimum, a factor of 3x improvement. The introduction of a dual ribbon thickness measurement capability with greater accuracy than ever before and better algorithms to control thickness have resulted in tighter thickness distributions for Gemini wafers than that seen in any earlier String Ribbon production data. In addition, design changes in the hot zone and improved thermal control have contributed to a better overall thickness distribution. This can be seen in one of the earlier distributions of wafer weight (= the wafer thickness) shown in Figure 15) for an earlier version of hot zone design, Gemini 1, and for the present one, Gemini 2. Note that the distribution is much tighter for the more recent development.

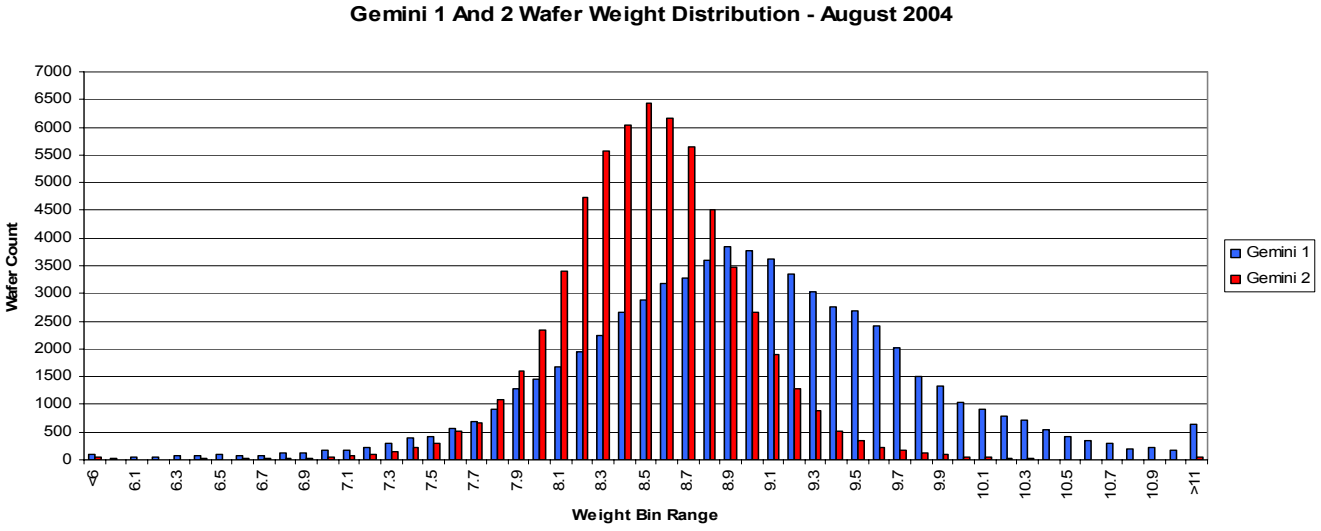

Figure 15 - Distribution of String Ribbon wafer weights following introduction of the improved thickness measurement and control systems (red) and prior to that (blue).

Melt Height

Melt depth or, as it is termed in Evergreen, “melt height”, is another important parameter that must be continuously monitored and controlled in an in-line fashion. The distance between the top of the melt and the solid-liquid interface is a highly sensitive parameter for satisfactory ribbon physical properties. Amongst other factors, as well, it can affect thickness uniformity, edge strength, and overall stress in the material.

An earlier finding was that the buildup of carbide in the bottom of the crucible would change the relative melt depth in the crucible. For example, if there was a 10 mil buildup of carbide, a melt height of 80 mils would mean that the top of the melt was actually 90 mils above the bottom of the crucible, and 10 mils closer to the top of the solid liquid interface. As a result, growth could be affected, leading to more losses due to cracking and edge breakout. By adding an offset which would modify the process variable as a function of the time, the melt height above the bottom of the virgin crucible could be calculated. This offset was a simple ramp function -algorithm, and was calibrated by measuring, as a function of time, the melt depth from the top of the arrangement used to control the meniscus.

Temperature measurement and control

A key element in better controls and, ultimately in-line diagnostics, is that of accurate temperature measurements in the growth crucible. In particular, the temperature at the feedstock replenishment end of the crucible, must be well controlled. Recently, an algorithm was developed that allowed for a two wavelength pyrometer to be employed such that the measurement was not sensitive to any dust or other such hot zone perturbations. The result has been an ability to lower the temperature of the replenishment end of the furnace by about 30^{o}C. This, then should result in lower dissolution rates of the graphite and less SiC forming – an important advantage in doing uninterrupted growth. Results are shown in Figure 16 below. The introduction of the algorithm occurred just before the temperature drop. All this work was done initially on the pilot line machines, and then transferred to the production furnaces.

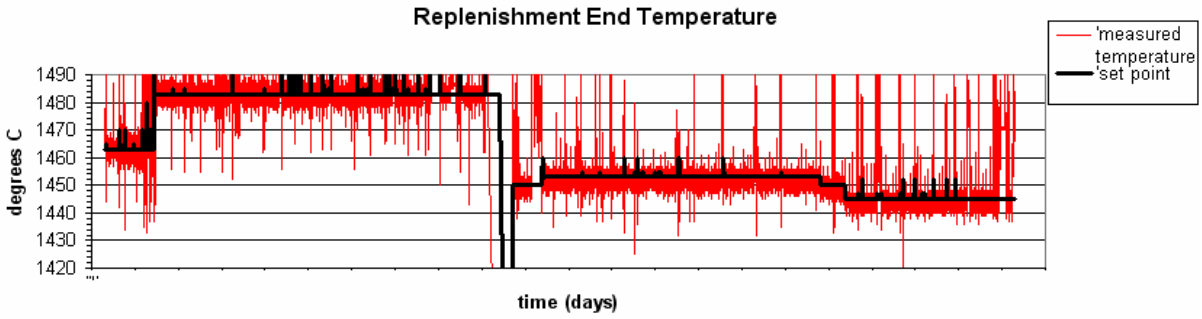

Figure 16 - Temperature of the feeder end of the crucible after the introduction of the algorithm for the improved pyrometer.

String tension

The following figure, Figure 17, shows how another parameter was improved through engineering design changes. In this case it was the string tension. The upper figure the shows the variation with time prior to the improvements introduced and the lower figure shows the reduced variation following the engineering improvements.

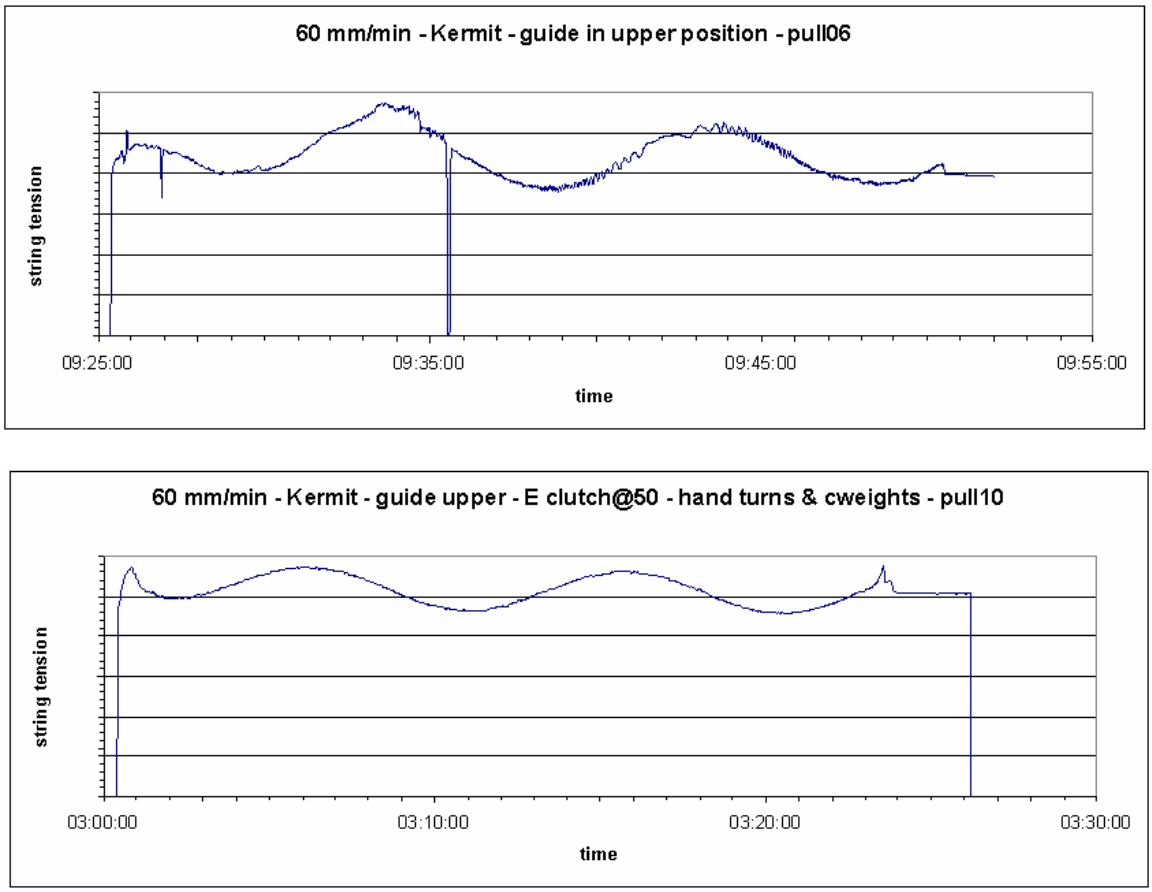

Figure 17 - Engineering improvements in String tension – upper curve before, lower curve, after the improvement.

Development of Centralized Computer Database of Downtime Reasons

A downtime analysis database was developed for manufacturing. Key features were an operator response screen on the PLC that would require the production operator to designate reason for stopping growth. This information was sent to database along with timestamp. Once growth was re-started, the non-growth time was automatically calculated for the event. This allowed for a finer analysis of reasons for each down time event and the typical duration for each type of event.

In-line diagnostics have been employed to create a more robust, easily reproduced ribbon machine. These improvements have yielded a 2x reduction in the start-up time for new growth machines. Methods for measuring melt temperature accurate to +/- 0.3^{o}C, a means for determining melt depth to +/- 8 microns and an in-situ thickness measurement technique that is accurate to +/-12 microns have all been developed and deployed in production.

The ability to grow dual ribbons from a single crucible means that many consumable costs, on a $/watt basis, can be virtually halved. The advances in controls and instrumentation indicated above have resulted in a significant increase in machine uptime and a concomitant increase in yield. Furthermore, the ribbon so produced is extremely flat, and this has improved downstream processing yields and made in-line processing that much more achievable.

Phase D – full production at a 15 MW/yr rate.

Two interlinked goals:

1. Full implementation of Gemini into an ultimately 15 MW/yr production rate

2. Total factory direct manufacturing cost reduction of 33%.

Sub tasks under goal #2 were these:

- Yield in crystal growth improved by at least 10%.
- Machine uptime increased by at least 10%
- # of crystal growth furnaces/ operator increased by 20%
- Overall factory yield increased by 10%

1. Full implementation of Gemini into an ultimately 15 MW/yr production rate

Following a successful pilot phase, the advances described above were incorporated into a final machine design and this was replicated throughout the production crystal growth area.

This was accomplished in two different ways. One was the conversion of existing crystal growth furnaces to Gemini and the other was by building completely new machines. The goal was 120 machines and, basically, this was met. Figure 18, below, shows a bird's eye view of the entire crystal growth production area with all Gemini furnaces.

Figure 18 – Aerial view of the production crystal growth area with all Gemini furnaces.

2. Total factory direct manufacturing cost reduction of 33%.

As will be seen, all goals were either met or exceeded.

Yield in crystal growth improved by at least 10%.

As the production area was fitted out with all the Gemini machines and operators became familiar with the running of these machines, yield steadily improved to the point where the goal of 10% was exceeded and a yield gain of 12% was obtained.

Machine uptime increased by at least 10%

Machine uptime also benefited greatly by the advances described above. Particular amongst these was the improved thermal control, the simpler and more modular hot zone design, and general advances in controls software. This goal was met.

Labor cost reduction

The number of crystal growth furnaces/ operator increased by 20%, thus resulting in a similair reduction in labor costs. The increased level of in-line diagnostics and the overall improved controls and instrumentation contributed to the attainment of this goal.

Overall factory yield increased by 10%

With the achievement of reaching the goals for the key production metrics, and, in addition given the flatness now achievable with Gemini ribbon, downstream yields in cell making and in module making were also improved. In particular, module yields were now excellent, with virtually no rejects after lamination. It took somewhat longer to reach this goal, but it also was attained in the end.

Bottom line for all the above is that the final goal of a direct manufacturing cost reduction of 33% has been met. This is a very significant achievement for Evergreen Solar.

Advanced cell making technology

The overall process used at Evergreen to make cells is as follows:

- Grow Gemini ribbons 2 m in length
- Laser cut into 15 cm long cell blanks
- Diffuse with P to form p-n junction
- Diffusant glass removal
- Silicon nitride deposition
- Back metal and front metal contacts applied
- Contact firing
- Cell test

Prior to diffusion, the 2m long Gemini strips are laser cut into 15 cm long solar cell blanks and stacked, using a robot, into a bar-coded plastic box. The last time there was any human (i.e. production operator) intervention was when the 2m long strips were laser cut. Following this the cut blanks are inspected automatically for any size variations and are weighed. The data shown in Figure 15 was obtained at this step. Figure 19 below shows the cell blanks are they are in a large pass-through between crystal growth and diffusion.

Figure 19 – Pass-through between crystal growth and diffusion.

Diffusion (a)

No-etch process

As already alluded to above, the development of Gemini was accompanied with improvements in the quality of the as-grown wafer surface. Prior to this, Evergreen had developed the so-called no-etch process in which wafers go directly from ribbon growth to cell processing without any intervening wet chemistry or etching. By eliminating a conventional process step between crystal growth and diffusion, yields are increased while process costs and acid waste disposal costs are reduced.

To define the process window of the ribbon surface oxide for the no-etch process, two sets of wafers were studied. The first set consisted of wafers taken from the crystal growth production line. Ellipsometery was used to measure d_{ox} at five points across each wafer, and the wafers were then processed with standard production diffusion conditions. The sheet resistance, ρ_s, was measured using four-point probe at the same locations as the thickness. The resulting data are shown below in Fig. 20

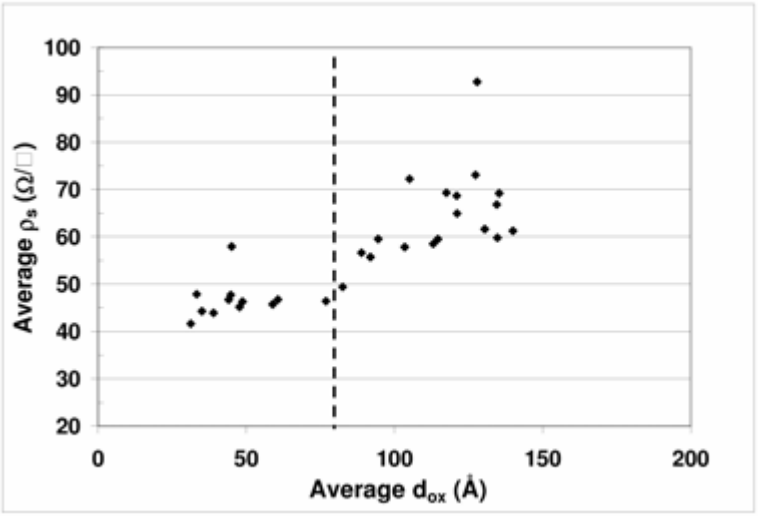

Figure 20 Dependence of sheet resistance on oxide thickness.

The sheet resistance is relatively insensitive to oxide thickness up to $\boldsymbol{d_{ox}}$ = 80Å, then rises more rapidly for thicker oxides. A similar trend is seen in the within-wafer uniformity of ρ_s as shown in Fig. 21. The standard deviation of ρ_s remains below 5Ω/□ up to $\boldsymbol{d_{ox}}$ = 80Å, then rises rapidly beyond that point. It is this increase in non-uniformity which defines the process window, because local regions with higher than average ρ_s lead to increased fill factor losses.

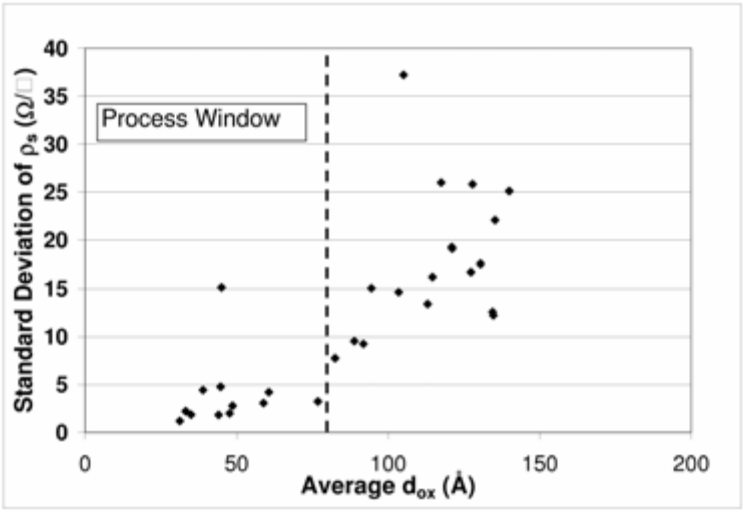

Figure 21– Within wafer uniformity of sheet rho.

Wafers with re-grown oxide

A second set of wafers was prepared with a different procedure to compare the surface oxide on as-grown wafers with a thermal oxide. In this test, the surface oxide was removed using HF. The wafers were then heated in a furnace in a dry air ambient to re-grow oxides of varying thickness. Some single-crystal Cz wafers with re-grown oxide and a few Gemini wafers with as-grown oxide were also included in this test for comparison. Oxide thickness was measured only at the wafer center, but ρ_s was measured over a nine-point grid. The ρ_s results for SR wafers with re-grown oxide are similar to those for SR wafers

with as-grown oxide (see Fig.22). The error bars show the standard deviation of the ρ_s measurements. Results for Cz wafers are similar to those for SR wafers at low oxide thickness. However, Cz wafers with thicker oxides show a different behavior than SR wafers: neither the mean value nor the standard deviation of ρ_s increases rapidly for d_{ox} > 80Å as they do in the case of SR wafers.

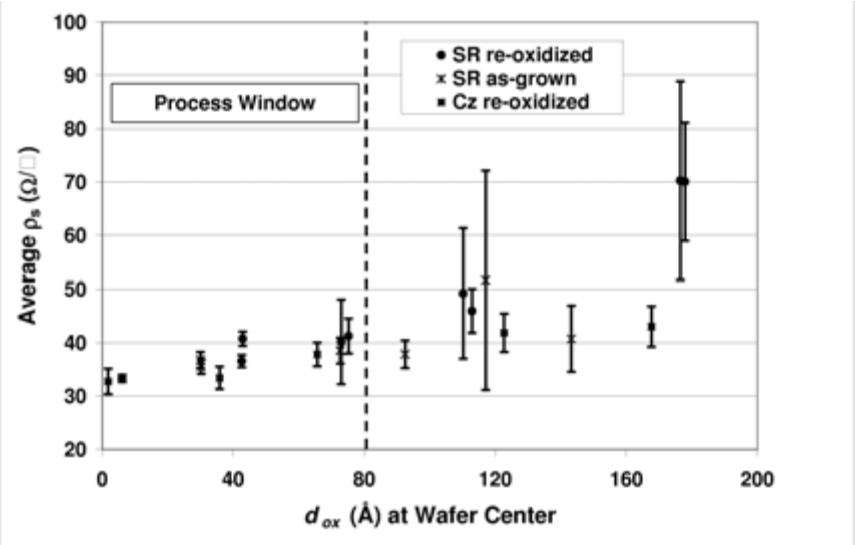

Figure 22- Sheet resistance vs. oxide thickness for SR wafers with re-grown and as-grown oxides.

Some of the wafers were also sent to NREL for SIMS analysis to obtain phosphorus doping profiles and are shown in Fig. 23. There is a linear decrease in phosphorus dose with increasing d_{ox} as is illustrated in Fig. 24**.** Because of limited availability of the SIMS instrument, most wafers were measured at only one spot, in the center of the wafer. Therefore, there is no data on non-uniformity of the dose to compare with the non-uniformity in ρ_s, and there is no obvious sign of the 80Å process window in these data.

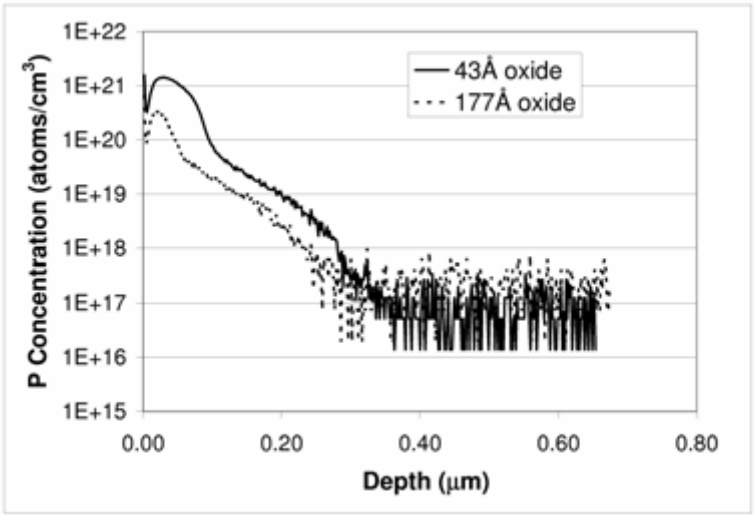

Figure 23 - Phosphorus depth profiles for two re-grown oxide thicknesses on String Ribbon wafers.

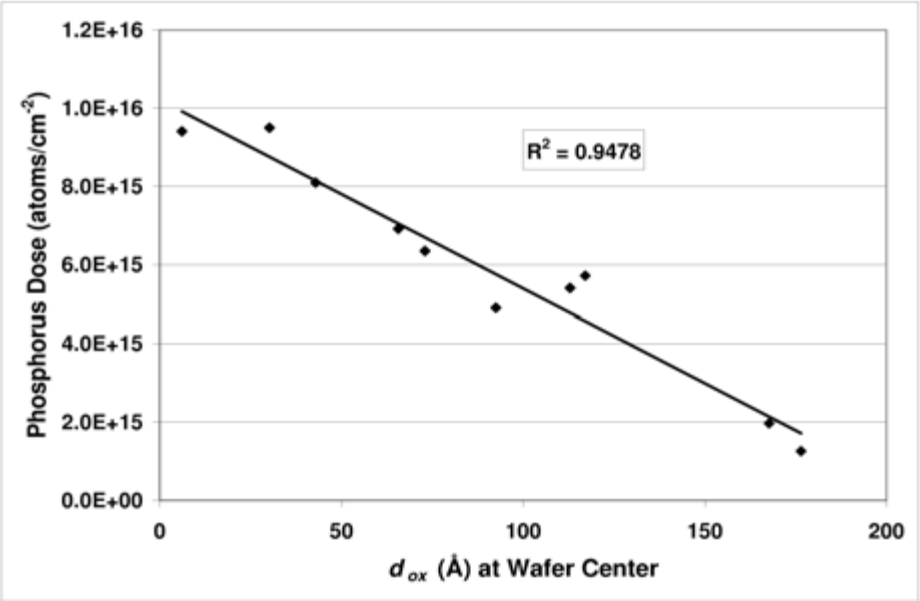

Figure 24 - Phosphorus dose vs. oxide thickness

Oxide thickness control

Gemini production furnaces over a two month period were followed in order to assess conformance with the process window defined above. Samples were measured at three to five points each on both sides of the wafer, including both front and back ribbons. The results are shown in Figure 25, with data points for the average of all furnaces and vertical error bars showing the standard deviation of the furnace averages.

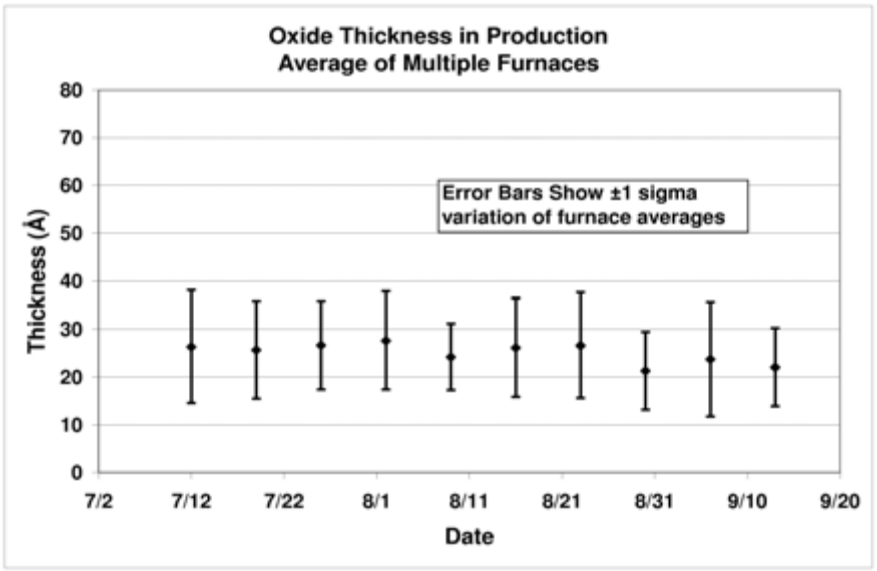

Figure 25 - Oxide thickness vs. date for pilot line of dual-ribbon production furnaces.

All the results were well within the 80Å process window. The average of all furnaces was between 20 and 30Å, and the standard deviation was 5-10Å. Establishing this level of d_{ox} control for such thin layers while simultaneously satisfying other constraints necessary for high-yield SR crystal growth represents a significant achievement attributable to superior furnace design of the Gemini system.

Inside and Outside Gemini Surfaces

A final test was that of any possible difference in the oxide layers on opposite sides of a Gemini ribbon. As already mentioned above in section xx, there is some expected ambient asymmetry with the inner and outer surfaces of the growing Gemini ribbons. Figure 26 below shows oxide thickness distributions for opposite sides ("inner" and "outer") of a Gemini wafer. These differences were not found to be statistically significant in terms of cell results.

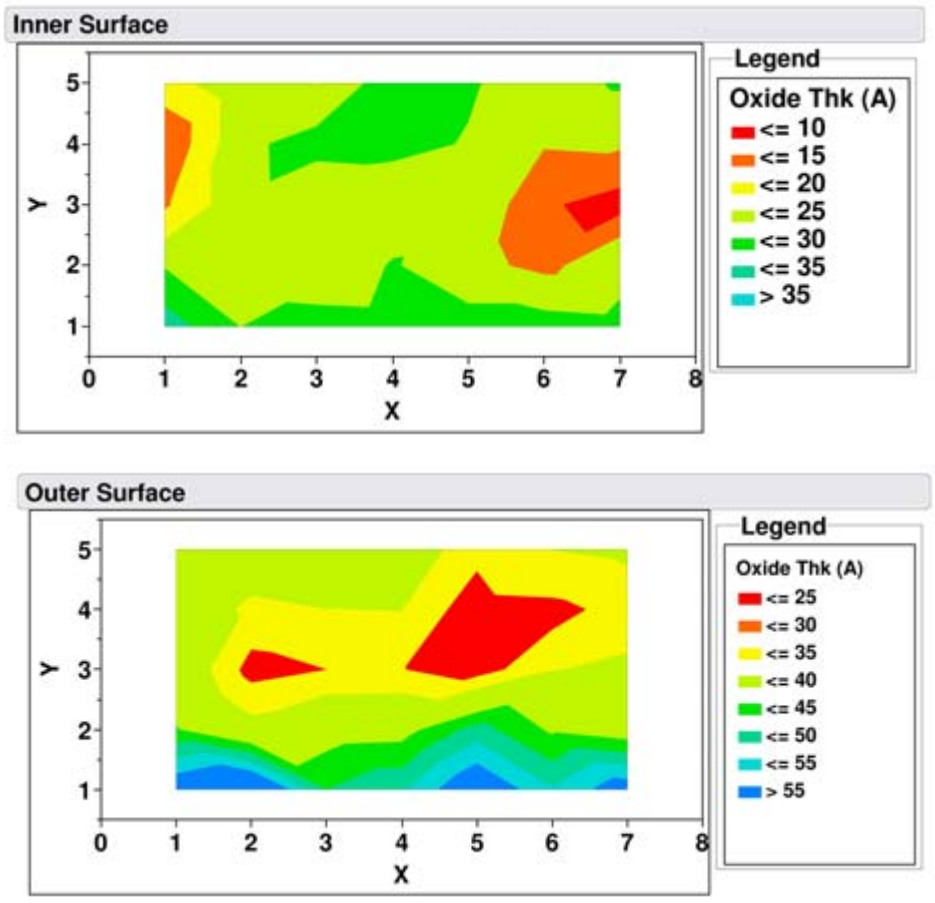

Figure 26 - Oxide thickness distribution for opposite sides of an as-grown Gemini ribbon

Diffusion (b)

The goal here was to develop a process and the associated equipment that would be compatible with the no-etch process and capable of high volume with low capital costs. An important part of the overall set up is that of the diffusant glass removal following diffusion. It was found that both the process and the equipment design for it were highly iterative. This is particularly so for String Ribbon Gemini wafers.

Robotic methods for loading and unloading wafers from bar coded boxes from crystal growth were developed and designed to run at rates of 8-10 MW/yr. These boxes then unload wafers into the diffusion area. The high volume diffusion set up has been run in production for some time with considerable success. It has been run at an annual rate of 10 – 15 MW. Diffusion uniformity is determined by periodic measurements of the sheet rho after diffusion and diffusant glass removal. A recent production report on sheet rho measurements made on selected wafers from the ten across scenario indicates that the sheet rhos average 48 ohms/sq. +4, -2 ohms/sq.

The machine to do diffusant glass removal following diffusion is an in-line machine custom made for String Ribbon wafers. There were several major concerns with the implementation of this machine in conjunction with the overall diffusion set up. One was whether an easy transfer could be effected going from the diffusion equipment to this glass etch machine. Another concern was yield through this machine - both mechanical (breakage) and efficacy of glass removal. The latter had two important implications. If some film is left on the wafer surface, then this could result in increased cosmetic yield rejects downstream. Further, a film on the surface prior to deposition of silicon nitride can adversely affect the nitride/passivation process.

Figure 27 shows the diffusant glass removal machine controls. The figure also shows wafers emerging from the machine prior to their being loaded into plastic boxes where they will then be transported to the silicon nitride deposition station.

Figure 27 - Diffusant glass removal station. Rows of cleaned, diffused cell blanks can be seen emerging from the machine.

Two parameters were found to be important here. One was the purity of the de-ionized water added to the HF and the other was the temperature of the HF bath. Adequate attention to each of these resulted in very uniform glass removal and film free surfaces following this step.

With suitable modifications to the mechanical aspects of the robotic loaders and unloaders and the diffusant glass etch machine, a high yield method to accomplish this was developed and successfully implemented.

Silicon Nitride

Loading and unloading

Robotic loading and unloading of the silicon nitride deposition equipment was designed so that wafers were robotically placed in boxes following diffusant glass removal. They were transported to the Silicon nitride deposition machine, unloaded by another robot and then loaded onto the nitride machine. This is shown in Figure 28.

Figure 28 - Robotic loading onto the silicon nitride deposition machine.

Coating uniformity

PECVD silicon nitride process is used both as an A.R. coating and for H passivation. Recent advances in the design of the apparatus that holds the wafers prior to deposition, have included a means to obtain tighter distribution of the silicon nitride thickness to improve yields and efficiency. Figure 29 shows some recent results.

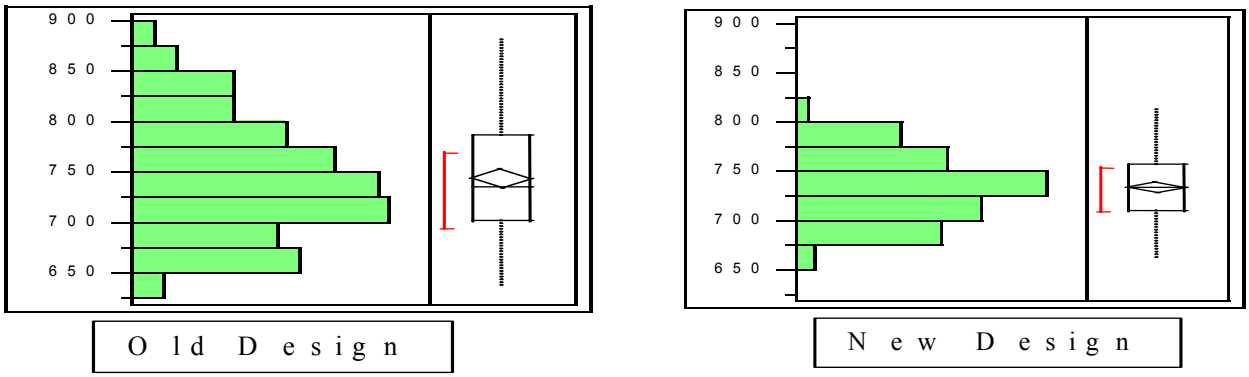

Figure 29– SiN thickness distribution with improved process using a new design.

Metallization

A proprietary method for forming metal contacts that results in less pressure on wafers than does conventional screen printing has been extensively developed at Evergreen. Earlier machines based on this method are not in-line and utilized a robot in a rotary configuration. For this project, it was decided to design a machine that would be in-line, scalable, and ultimately represent a basic unit size in terms of yearly output and reproduction for future expansions. The initial machine was prototyped in the lab, the concept verified, and a single, in-line machine was built, debugged and run in production. A portion of it is shown in Figure 30. This machine was designed so that multiple lines could be run on it. Consequently, after about a year of production experience with the single, in-line machine, a second line was built onto the machine, giving it a total capacity of 8-10 MW/yr.

Figure 30 – In-line front contact application machine

One of the outstanding features of the Gemini wafers is that they are flatter than any prior ribbon grown at Evergreen. This has had important implications in cell processing yield. With the flatter Gemini wafers, and the machines described above, a 6% increase in cell processing yields has been realized. Figure 31 shows robotic positioning of a metallized cell prior to being tested. The rose colored light is used to help the vision system find the edges of the cell.

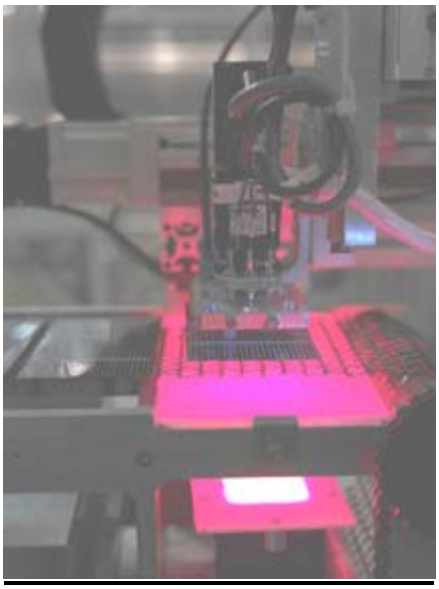

Figure 31 - Robotic positioning of a metallized cell prior to being tested

Efficiency

Lifetime

Minority carrier lifetime of the as-grown ribbon has been addressed in several different ways. Enhanced purification of the graphite crucibles has been shown to be helpful here and this is illustrated in Figure 32. The horizontal scale in this figure is time. The graphite is purified by heating it at temperatures above 2000^{o}C under a halogen. Volatile metallic halides are then removed in this purification process. The uptick in lifetime value corresponds to the time when the improved purification process was implemented.

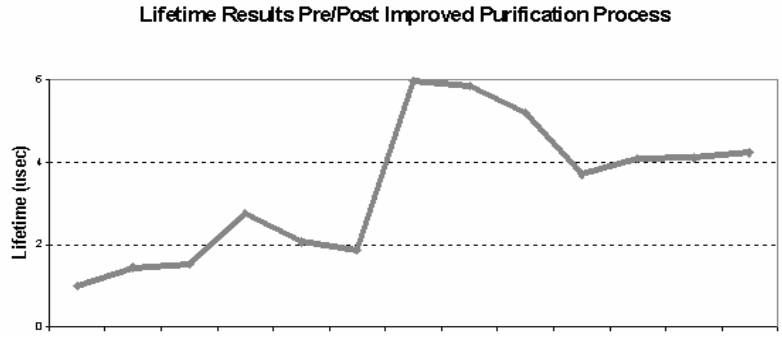

Figure 32 – Lifetime improvements with an enhanced graphite purification process.

This improvement also manifested itself in an increase in the short circuit current of about 4%.

Efficiency effect due to run length in crystal growth.

As mentioned above, Gemini II has been characterized by long run lengths. That is, long periods of time before a growth crucible needs to be replaced. As a consequence, the effect of run length on efficiency was studied, as there was some concern of a drop in efficiency with these long run lengths, possibly due to increased impurity build-up in the melt.

A single Gemini II furnace was chosen for this experiment. The wafers were stored in a cabinet at ambient conditions in the diffusion area until the entire run was completed. They were then divided into three lots corresponding to the beginning, middle, and end of the run. Two wafers were selected from each lot for physical and electrical analysis.

All three lots were processed together in cell fab. Cell test results for the three lots are summarized in Figs. 33a-c below. Outliers have been removed from the data. The red boxes on the plots show the quantile ranges or distribution of the data, with the median at the location of the line at the center of the red box.

Figure 33a shows the efficiency comparison of the three lots. It can be seen that quite a few cells were at 14.2% or better, but that the median was just below 14%. The median efficiency declined from nearly 14% in the first third of the run to 13.65% in the last third of the run. Other quantiles showed similar changes, indicating that the entire distribution shifted lower.

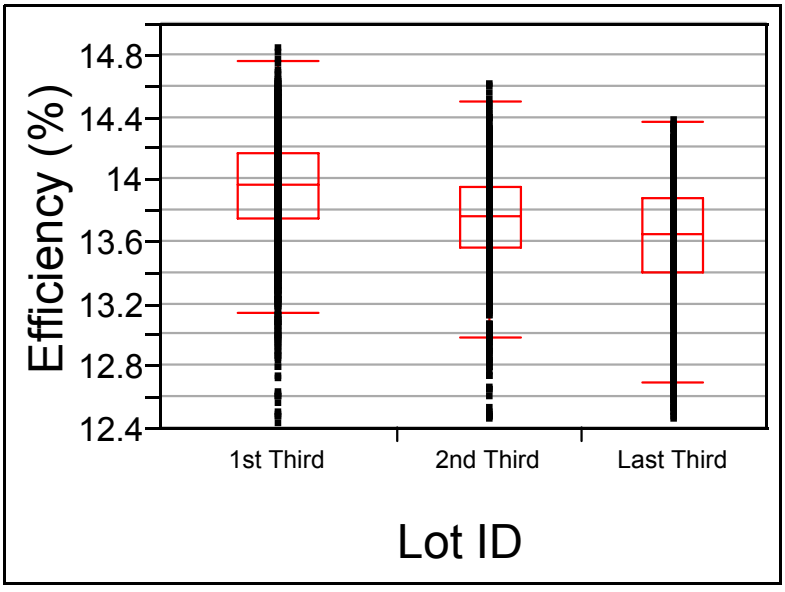

Figure 33a - Efficiency vs. Run Length

The initial hypothesis was that efficiency changes would be driven by accumulation of impurities in the crucible over the extended run length. If correct, this effect would be expected to depress Isc. However, the percentage change in Isc was less than that observed for the efficiency. The results for Isc are shown below in Fig. 33b.

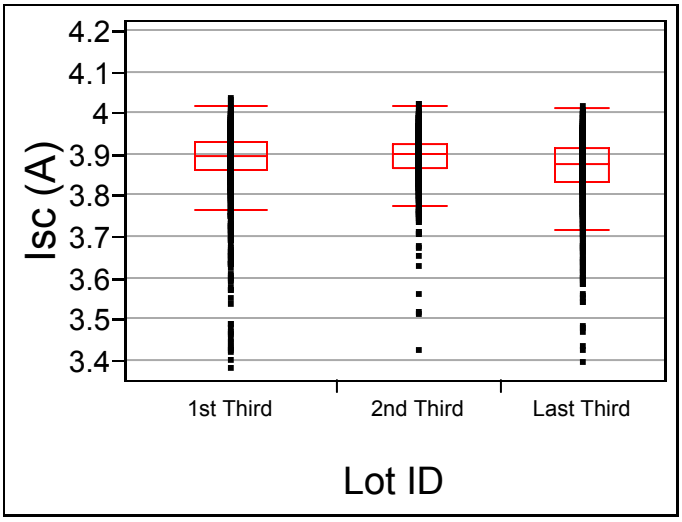

Figure 33b - Isc vs. Run Length

Isc was unchanged from the 1st third of the run to the 2nd third. In the last third, Isc declined by 0.5% relative to its original value. This would account for an absolute efficiency change of only 0.08%, much less than the total drop in efficiency observed. This result indicates that accumulation of impurities does not appear to be a dominant effect. The rest of the efficiency drop is attributable to a decrease in the fill factor, as shown in Fig. 33c below. The change in Voc was approximately 0.3%, the smallest component of the efficiency change.

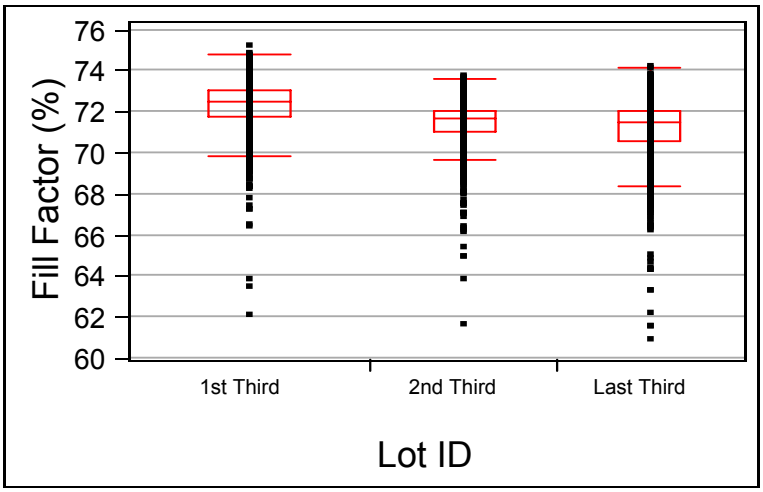

Figure 33c - Fill factor changes with run length

The median fill factor decreased from 72.5% to 71.5% over the length of the run. This change corresponds to a 1% (abs.) decrease, accounting for close to 0.2%(abs.) of the efficiency loss. One

possible explanation for the change in fill factor would be changes in the oxide thickness on the as-grown wafers, but it was not possible to obtain a statistically meaningful sampling of such large lots given the time required for the oxide measurements.

Based on the above, it seems likely that the change reflects process variation in cell fab which has nothing to do with furnace run length. The front contacts were changed between the 1st third lot and the other two lots. However, the contact qualification lots showed fill factors of 71.7% and 71.3%, a change of only 0.4% (abs.) Therefore, the change in contacts can account for only 40% of the fill factor decrease. The rest of the fill factor decrease remains unaccounted for. Since the different wafer groups were stored for varying lengths of time (from days to weeks) in the ambient factory conditions, it is also possible that these storage conditions had some effect on the results.
The relative contribution of the Voc, Isc, and FF changes are shown in Figure 34 below.

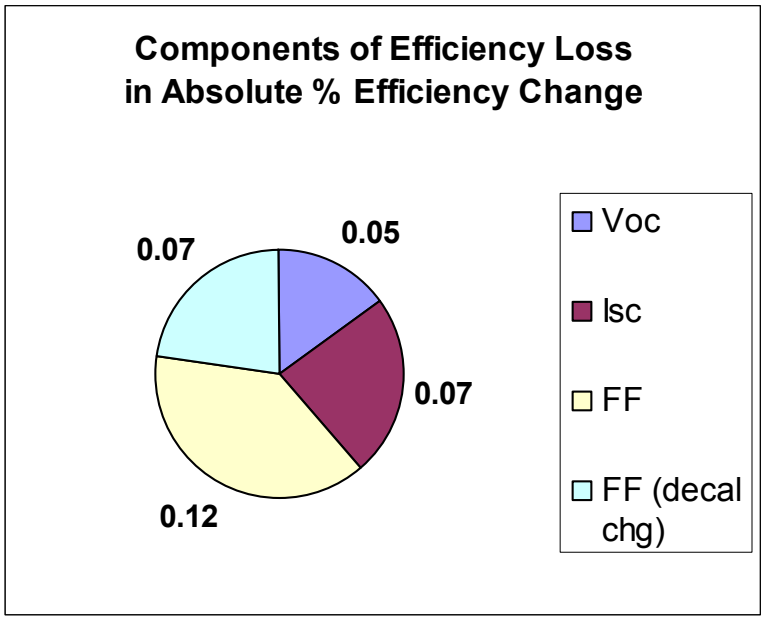

Figure 34 - Contribution of Various Factors to Overall Efficiency Loss

Conclusions on run length experiment

The efficiency for Gemini cells was observed to decline by approximately 0.32%(abs) over a long crystal growth run length. However, the drop in Isc accounted for approximately 0.07%(abs) of the efficiency change. The dominant factor driving the efficiency decrease was the fill factor. About 0.07%(abs.) of the FF-related efficiency drop was probably caused by a change in front contacts which occurred while the test lots were being processed. The root cause of the remaining efficiency loss is unknown for certain but may be due to variations in the cell processing area.

Improved front contact design

It has been evident for some time that the proprietary method used at Evergreen to make metallization contacts could be improved. Recent work has focused on the front contact. The approach taken is to develop a drop-in improvement for production that will represent a minimal disruption for the line. As a

result, the number of metallization fingers will initially be kept constant but with efforts to make taller and narrower fingers. This approach has resulted in a closer look at the temperature and chemistry involved in the front contact formation process. A lower temperature and modifications in the chemistry have already produced some promising results as is shown in the following figures. Figure 35 shows a cross section of a typical SOP Ag front contact finger. In this case the cross sectional area is 1700 sq. microns. In figure 36 below, a taller and narrower finger of almost equivalent total cross section of 1624 sq. microns is shown.

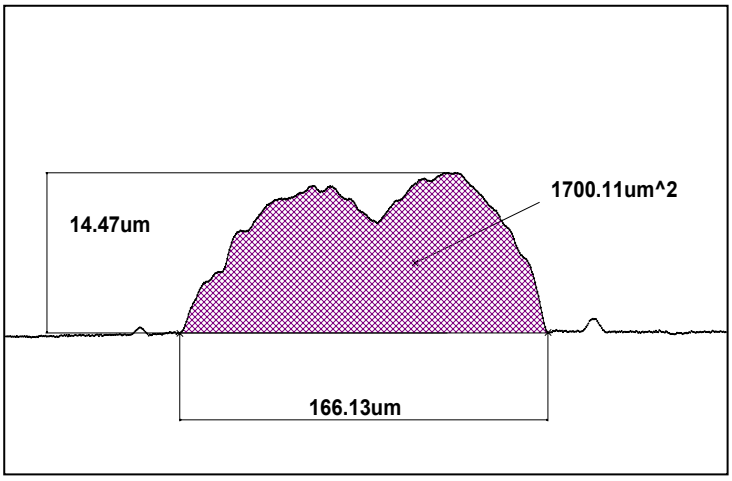

Figure 35 – Cross section of an SOP front contact finger.

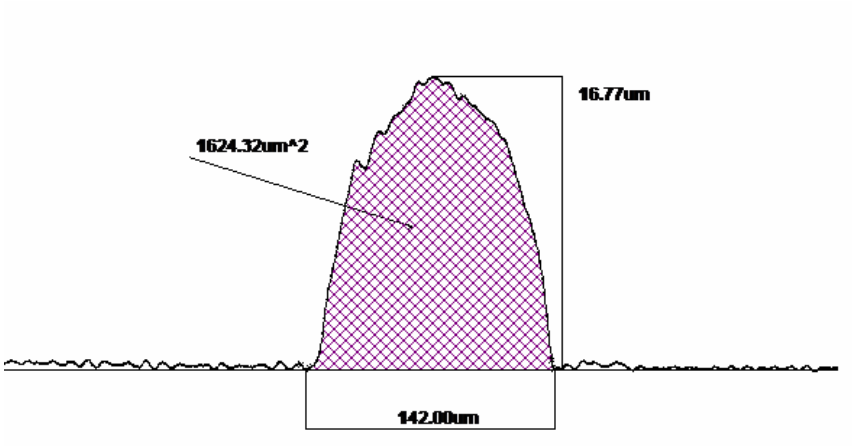

Figure 36 – Cross sectional area of a taller and narrower finger.

The issue with all these results is that the contact resistance goes up with narrow fingers and the overall expected gain is then not realized. This may be related to excess carbon present at the silicon – Ag interface that then reduces some of the glass frit in the Ag paste.

Efficiency for production batches

Figure 37 shows the efficiency distribution for a high efficiency batch of production wafers. Note that the best efficiencies are at the 14.5% level. Efforts at quantifying why the distribution is as wide as it is, particularly the low end of the distribution, and how to make more cells in the 14-14.5% range have

centered on three areas: starting lifetime, wafer thickness uniformity, and higher sheet rhos in diffusion. In the earlier section on Gemini ribbon growth thickness control was discussed and it was shown how this has been improved very significantly. The other two areas are still under active investigation.

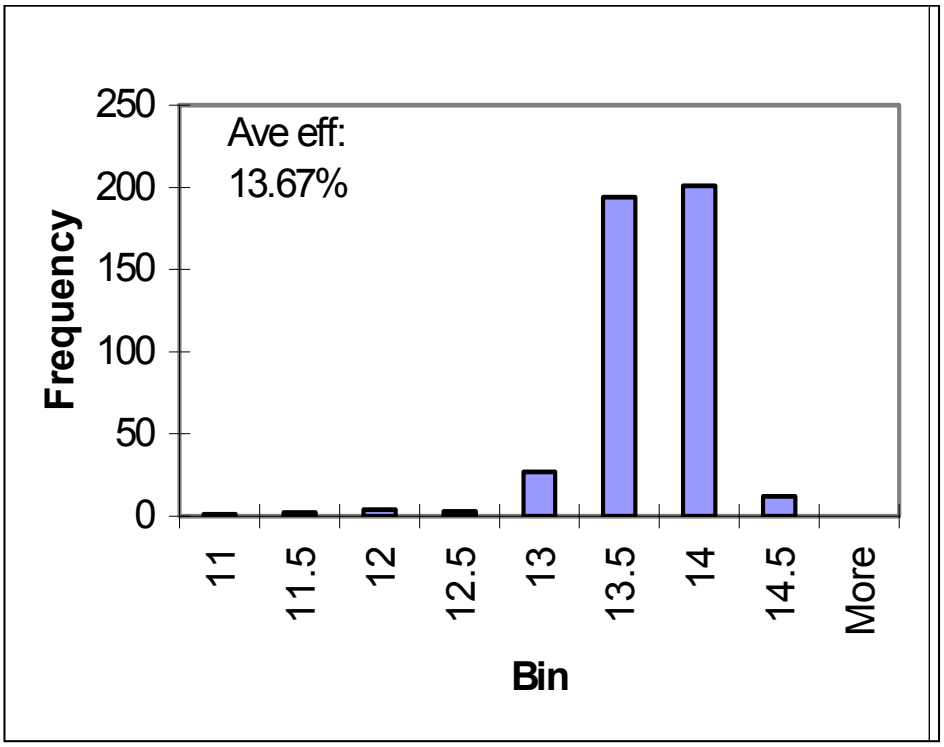

Figure 37 - Efficiency distribution for a high efficiency batch of production wafers.

Interaction with Georgia Tech

As part of the overall efficiency studies in this project, Evergreen has worked closely with Prof. Rohatgi's group at Georgia Tech.
They have recently done some LBIC scans of four cells with varying Jsc values as shown in Figure 38 below. The purpose here was to try to identify the reasons for the difference in Jsc values for the four cells.

These scans clearly indicate that a few bad regions (the darker regions in the scans) in the cell can bring down the overall value of Jsc. Additional characterization of the surface reflectance of our nitride layer for these four cells was done and is shown in Figure 39.

While very informative, this characterization work did not answer the question of why there were differences in the Jsc values for the four cells other than the fact that there was more recombination in the cells with lower Jsc values.

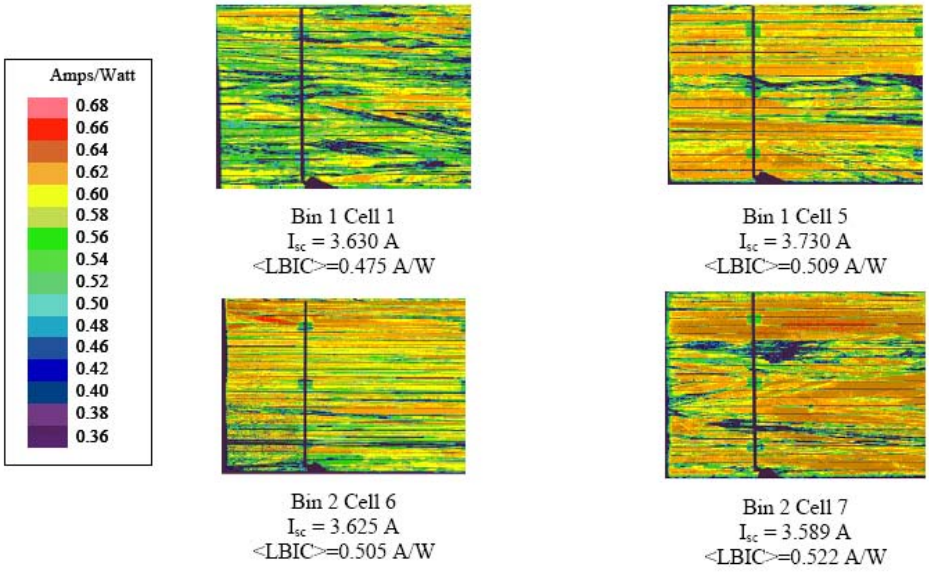

- LBIC scans were made using the PVSCAN 5000 system with a 980 nm laser.
- There is no evidence that the distribution of electrically active defects is related to the bin number.
- LBIC response decreases over the silver contact pads on the rear of the cell, presumably due to a local increase of the back surface recombination velocity at the silver/silicon interface

Figure 38 –LBIC scans for four wafers with varying values of Jsc.

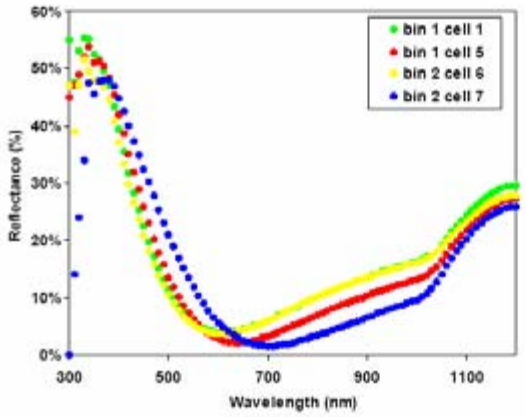

Cell	Average Weighted Refleactance 300-1000 nm (%)
bin 1 cell 1	12.3
bin 1 cell 5	10.8
bin 2 cell 6	11.8
bin 2 cell 7	11.0

- Reflectance was measured on one point of each cell using a white light source and monochromator and an integrating sphere
- Significant distribution in reflectance curves for each cell was observed and is also apparent in the average weighted reflectance
- Reflectance of cells did not show a clear dependence on bin number
- Variation in the average weighted reflectance values in these cells could cause a variation in J_{sc} of 0.5 mA/cm^2

Figure 39 – Reflectance measurements for the four cells in Figure 38.

Another important aspect of the Georgia Tech work is that it has also been shown that very high final, processed lifetimes, on the order of 50 – 100 microseconds, can be obtained on String Ribbon when RTP methods are applied to it. This augurs well for future efficiency gains with String Ribbon.

Monolithic Module Development

As already mentioned, at the outset of this three year subcontract, a major focus was on the development of monolithic module technology. During the second year, the Gemini project became a far more dominant project and the decision was made to concentrate on it and to phase out the monolithic module work. The following will summarize the status of this work by the end of this second year.

The rationale behind the monolithic module concept is that of eliminating the conventional front to back interconnection as is now practiced by virtually all manufacturers of crystalline silicon solar cells. This step as now practiced, requires considerable equipment design, is more difficult with thinner wafers, and, in general, is one of the lower yield steps in the overall module making process.

The monolithic module also requires cells that have all the contacts on the rear surface of the cell. The concept is shown is shown in Figures 40.. Figure 40 also shows the use of wrap-around contact cells in a monolithic module. The dark lines in the lower portion of Figure 40 indicate a conductive adhesive that is printed on the backskin material, and this will be discussed at length further in this section.

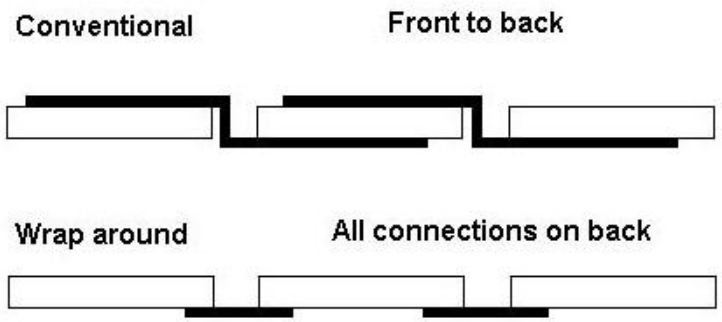

Figure 40 - Showing how a module made with wrap-around cells would differ in interconnection from a module made in the conventional way.

Formation of wrap-around contacts

This proved to be a difficult task in this project. Much of the difficulty was due to the early Gemini cells that were available for this work. These cells were made on material that was not nearly as flat as the later Gemini ribbon. This lack of flatness resulted in difficulties in attaching a cell with a wrap-around contact to the conductive adhesive bars that were printed on the backskin material. If the ribbon was not flat, then encapsulant from the front of the cells would flow behind the cells and prevent the formation of a good contact between the conductive adhesive bars and the wrap-around contact. This effect was confirmed by utilizing cast polycrystalline wafers and demonstrating that the flatness they possessed allowed for a suitable contact to the conductive adhesive bars. It is felt that using the present, much flatter Gemini wafers would obviate this problem, but this was not tested. The wrap-around edge in the early work was the long edge of the cell. This is the edge that contains the string used in the String Ribbon growth process. As will be shown further, using the laser cut, shorter edge of the String Ribbon cell was found to be a better way to form the wrap-around contact when, only half of a usual cell is used. That is, a cell that is 8 cm x 7.5 cm instead of 8 cm x 15 cm.

Efficiency of wrap-around cells

Not surprisingly, there is some loss of current due to leakage around the edge where the wrap occurs. The result is efficiencies that, to date, at least, trail those of conventional cells. Example of one of the

best cells (bottom row) and more typical cells are shown in the following Figure 41. The cells are all 60 cm^2 in area.

typical

Voc	Jsc	Vmax	Imax	Pmax	FF	Eff.
0.587	31.98	0.462	1.683	0.778	0.69	12.96%
0.590	32.11	0.469	1.737	0.814	0.72	13.57%

Figure 41 - Efficiencies for wrap-around contact cells

Second layer encapsulant issue

One of the key issues in forming a monolithic module with back contacted cells is how to satisfy the presumed need for an encapsulant layer behind the cells and not have such a layer interfere with forming the contacts in the rear. The encapsulant layer is a non-conductive polymer. In the conventional method for making modules, there are two encapsulant layers, one between the front of the cells and the superstrate glass and one behind the cells, between the rear of the cells and the backskin of the module.

An elegant solution to this problem of an encapsulant behind the cells in a monolithic configuration has been obtained with the use of Evergreen's proprietary backskin material. This backskin material bonds directly to the back of a solar cell and therefore completely obviates the need for a second encapsulant layer behind the cells.

Overall layout for a monolithic module

Figure 42 below shows the overall layout for a monolithic module using wrap-around cells. The backskin material with the printed bars of conductive adhesive is at the bottom, the wrap-around cells are shown in blue, a transparent encapsulant layer and finally a superstrate of glass are shown.

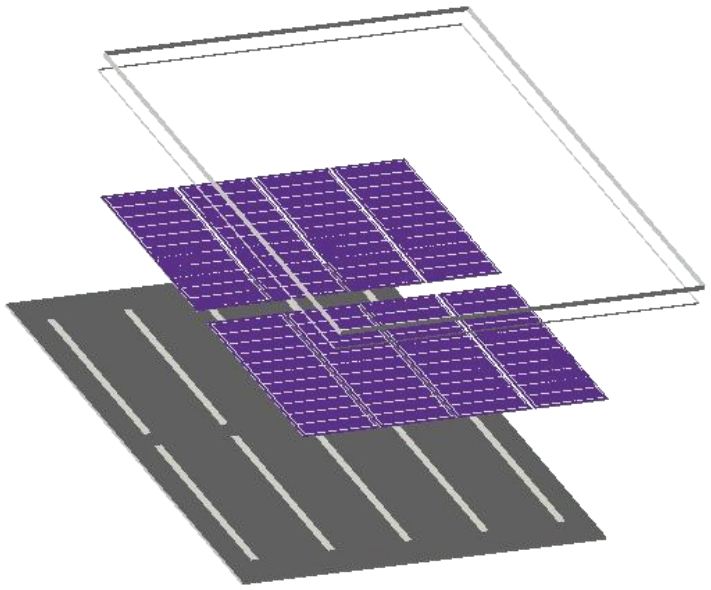

Figure 42 – Showing the layout of a monolithic module. The backskin material with the printed bars of conductive adhesive is at the bottom, the wrap-around cells are shown in blue, a transparent encapsulant layer and finally a superstrate of glass are shown.

Forming wrap-around contacts

An in-line machine for forming wrap-around contacts was modified and used as the basis for a production machine to form contacts on conventional (not wrap-around) String Ribbon cells. This machine is now capable of forming contacts at a 10 MW/yr rate, operates on an in-line basis, and is a key element in Evergreen's overall expansion plans. A picture is shown in Figure xx in the solar cell section above.

Backskin shrinkage issue

The backskin material used for forming monolithic modules is the proprietary material originally developed under the first PVMaT project at Evergreen. For use in a monolithic module, an issue that emerged with its use was that of shrinkage. As shown in Figure 42, a series of conductive adhesive bars are printed onto this backskin material. Given this, it is important that the spacing between the bars is maintained – that is, dimensional stability is needed here. Sheet extruded polymers can exhibit shrinkage in the extrusion direction. The shrinkage occurs when the polymer is heated and the polymer chains that were stretched in the extrusion direction tend to relax. The easiest way to handle this problem is to heat the backskin before the conductive adhesive contacts are printed on it. Some work was done on a roll to roll method to do this with I.R. heaters between the two sets of rolls. The speed of the rollers following the heated region was adjusted to allow for the shrinkage of the polymer. Although this was part of the original plan, a production type machine for this, was, in the end, not built. This was partly due to the fact that the close-out of this particular project was already a likely possibility. Instead, a batch type process was used and was found to be satisfactory for the smaller quantity of modules that were made.

Development of a suitable conductive adhesive

This was one of the largest technical challenges of this part of the project. There are a large variety of commercially available conductive adhesives. The key here was to find one that had sufficient conductivity, could be printed easily onto the backskin, would form a good contact with the wrap-around cells, be cost-effective, and finally, hold up under repeated thermal cycling. The latter requirement is generally viewed as the most important criterion to satisfy in terms of forming a long, term reliable module. As will be shown at the end of this section, the final material chosen for this purpose satisfies all the requirements very well.

Method to make monolithic modules

The technique involved three principal areas that are then broken down into the following steps:

1. Wrap-around contact cells
    a. Form wrap-around contacts using in-line metallization application machine to apply front contacts
    b. Apply the rear contact using in-line metallization application machine.
    c. Fire cells.
    d. Test and bin cells.

2. Backskin
    a. Cut backskin sheets to size and pre-shrink.
    b. Print conductive adhesive bars.

3. Monolithic module construction
    a. Place wrap-around contact cells onto backskin.
    b. Form external contacts and module edging.
    c. Laminate
    d. Trim
    e. Module test.

Several different designs of modules were studied. This included modules with a molded frame and the leads molded as well – 55 W size modules were constructed this way. Another type module was one that

was not molded, it was 25 W in size and had bare edges. Figure 43 shows a sheet of the backskin material with bars of the conductive adhesive pattern that has been printed on it. The size if this particular sheet is that to form a 55 W module. The backskin material is 40 mils thick and was pre-shrunk before the pattern was printed on it. The conductive adhesive bars are spaced in this case to accommodate an 8 cm wide x 15 cm long String Ribbon solar cell.

Figure 43 - Backskin sheet for a 55W size module.

An issue with forming the monolithic module that had a molded edge and molded in leads was that of the external leads and the sealing of these to the polymer edging. Some of the early accelerated tests, particularly thermal cycling, indicated that an electrical failure could occur in this portion of the module. Figures 44 and 45 show the front and rear of such a region.

Figure 44 – Top front of a monolithic module showing the region where the leads emerge from the module.

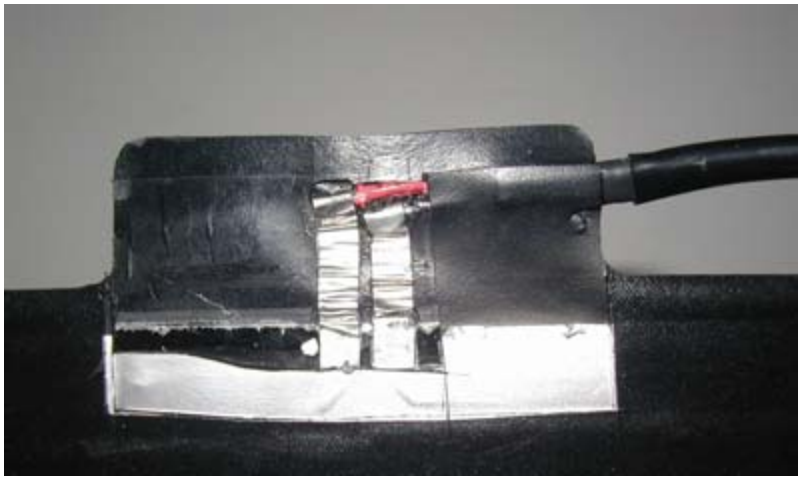

Figure 45 – Rear of the top front of the module shown in Figure 44, with the backskin covering cut away to reveal the connections to the external wire.

These photographs show detail of the leads emerging from a monolithic module with a polymer frame and sealed leads. In Figure 45, the back covering to seal the leads has been removed to show how the leads from the module connect into the wire that becomes the external wire of the module. A long term failure mode can be seen in the leads coming from the module. They show severe crimping – a result of thermal cycling. This crimping can result in a short and a module failure. The issue of crimping was successfully addressed by using the appropriate polymers in the region of the connection to the external wire and insuring that the crimping shown in Figure 45 above would not then occur. A method to incorporate the placement of these polymers in some sort of automated machine and procedure was not developed but it was felt that this could be done when required.

55 W size modules were made initially with String Ribbon cells and also with cast wafers cut to the size of String Ribbon wafers, i.e. 8 cm x 15 cm. An example of such a molded module with String Ribbon cells is shown in Figure 46.

Figure 46 - Example of a 55 W size monolithic module with molded edges and leads.

As mentioned above, the early work with String Ribbon wafers encountered a problem with wafers that were not sufficiently flat. The result of this was that 55W sized modules made with String Ribbon cells did not hold up well in thermal cycling tests. However, two modules were also made using flatter, cast wafers and these were fine after 200 thermal cycles.

25 W size modules

Figure 47 below shows a typical 25 W monolithic module made with wrap-around contact cells that are 60 cm^2 in area. Note that these modules had no edging whatsoever. A coffee cup is in the lower left side of the picture in order to give a sense of the module size.

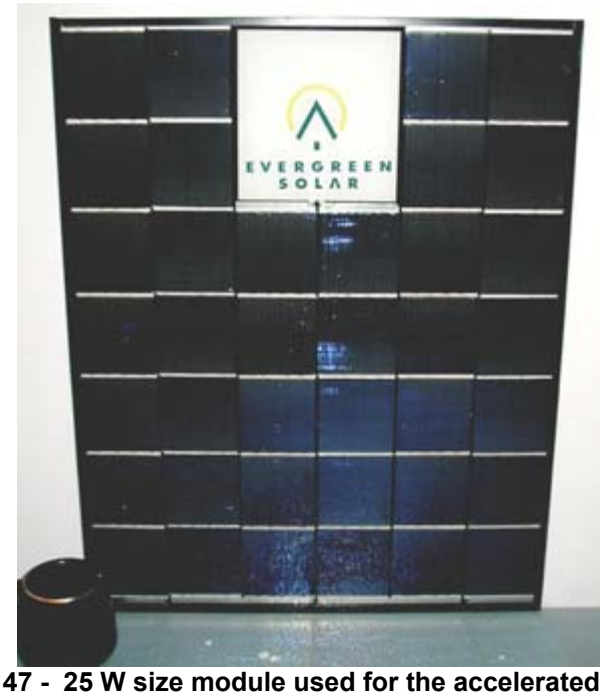

Figure 47 - 25 W size module used for the accelerated testing.

An I-V curve for one of these 25 W size modules is shown in Figure 48.

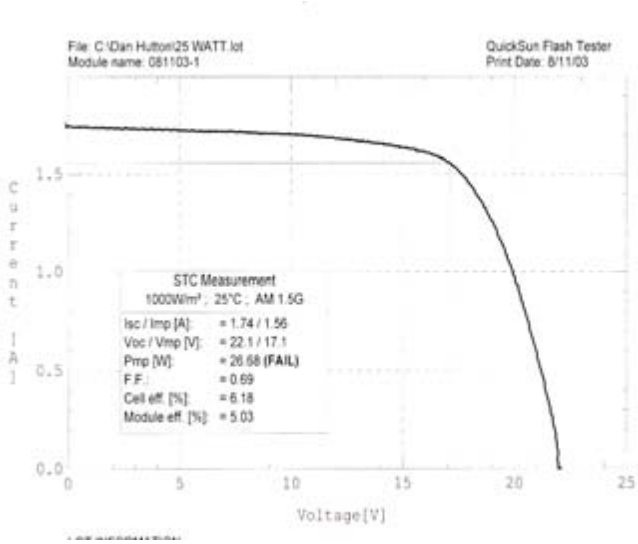

Figure 48 - I –V curve for a 25 W monolithic module

The key item to notice is that the fill factor for the module is better than ever before, at 0.69. It is believed that this is due to lower series resistance of the overall module and this is due to improved printing of the conductive adhesive bars on the backskin material. (the designation “fail” for the peak power value is meaningless - it is an artifact of the module tester.) Of course, as conventional modules go, this is still low for the fill factor. There is still room for improvement here.

Accelerated Testing

One of the earliest concerns with the overall monolithic module scheme is that of the long term integrity of the wrap-around contacts to the conductive adhesive bars printed on the backskin. Thus, once a module construction was settled on, the focus shifted to doing thermal cycling to test the integrity of this bond.

The data in Figure 49 was generated from small (25 W size) monolithic modules that were subjected to thermal cycles until failure. These modules did not have a polymer edging or any edge protection at all. Instead, they had just a bare edge. As a result, the only failure mode seen was delam after the very large number of thermal cycles. Each color or symbol represents a different module. As can be seen, a number of modules went out to over 1600 cycles without any power changes greater than +/- 8%. It should be noted that the qual tests require a power drop of less than 10% after 200 thermal cycles.

This is a highly significant result. It means that the conductive adhesive/backskin combination along with wrap-around contacts could be quite viable from the point of view of long term reliability.

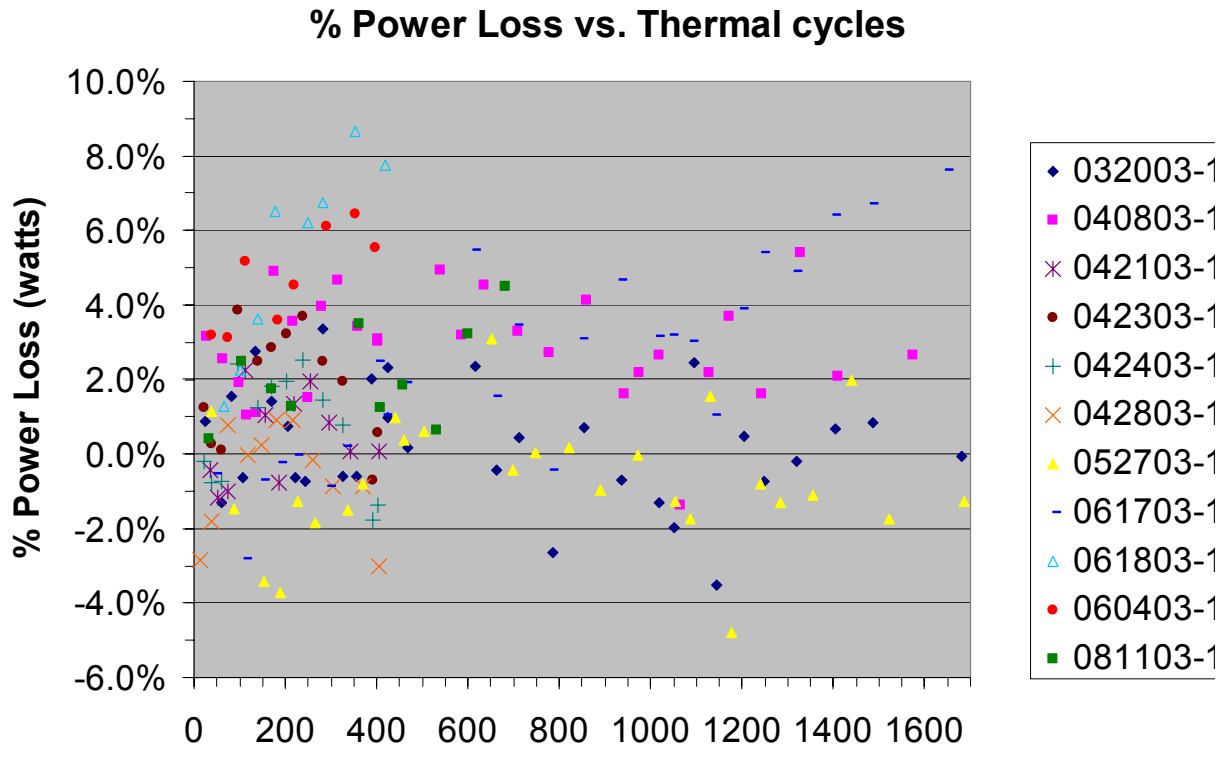

Figure 49 – Thermal cycle data for monolithic modules

SUMMARY

A three year PV Manufacturing Research and Development subcontract has resulted in major gains for Evergreen Solar. As a result of this work, Evergreen is now poised to take String Ribbon technology to new heights. In the ribbon growth area, project Gemini – the growth of dual ribbons from a single crucible-has reached or exceeded all the manufacturing goals set for it. This project grew from an R&D concept to a production pilot phase and finally to a full production phase, all within the span of this subcontract. A major aspect of the overall effort was the introduction of controls and instrumentation as in-line diagnostic tools.

In the ribbon production area, the result has been a 12% increase in yields, a 10% increase in machine uptime, and the flattest ribbon ever grown at Evergreen. In the cell area, advances in process development and robotic handling of Gemini wafers have contributed, along with the advances in crystal growth, to a yield improvement of 6%. Particularly noteworthy in the cell area was the refinement of the no-etch process whereby the as-grown ribbon surface could be controlled sufficiently to allow this process to succeed as well as it has. This process obviates any need for wet chemistry or etching between ribbon growth and diffusion.

Evergreen's factory in Marlboro, MA, has expanded to a maximal capacity of about 15 MW/yr. The net result of all of this has been a reduction of 33% in direct manufacturing costs, a very notable achievement.

Earlier in the project, the focus was on monolithic module development. With the Gemini advances described above, the focus of the entire project changed and the monolithic module work was brought to a close during this second year of the overall three year project. A significant advance in this technology was the development of a conductive adhesive in combination with Evergreen's proprietary backskin and encapsulant. 25 W size experimental monolithic modules have been tested and found to able to withstand up to 1600 thermal cycles.

ACKNOWLEDGEMENTS

A large number of Evergreen Solar employees have contributed to this work. In alphabetical order they are:

Dr. Andrew Anselmo, Dr. Bob Clark-Phelps, Mary Cretella, Scott Danielson, Dr. Chris Dube, Joe Fava, Tom Ford, Dr. Andrew Gabor, Leo van Glabbeek, David Harvey, Dan Hutton, Rob Janoch, Peter Kane, Dick Krauchune, Jennifer Martz, Jack McCaffrey, Roger Newman, Alan Rolke, Mike Ralli, Carolyn Schad, and Rick Wallace.

The support of NREL under Subcontract No. ZDO-2-30628-09 in general and our technical monitor, Katie Brown, in particular, is gratefully acknowledged.

REPORT DOCUMENTATION PAGE

Form Approved
OMB No. 0704-0188

PLEASE DO NOT RETURN YOUR FORM TO THE ABOVE ORGANIZATION.

1. REPORT DATE *(DD-MM-YYYY)*	2. REPORT TYPE	3. DATES COVERED *(From - To)*
October 2005	Subcontract Report	March 2002 – January 2005

4. TITLE AND SUBTITLE
Innovative Approaches to Low-Cost Module Manufacturing of String Ribbon Si PV Modules; Final Subcontract Report, March 2002 – January 2005

5a. CONTRACT NUMBER
DE-AC36-99-GO10337

5b. GRANT NUMBER

5c. PROGRAM ELEMENT NUMBER

6. AUTHOR(S)
J.I. Hanoka

5d. PROJECT NUMBER
NREL/SR-520-38679

5e. TASK NUMBER
PVB56101

5f. WORK UNIT NUMBER

7. PERFORMING ORGANIZATION NAME(S) AND ADDRESS(ES)
Evergreen Solar, Inc.
259 Cedar Hill Street
Marlboro, MA 01752

8. PERFORMING ORGANIZATION REPORT NUMBER
ZDO-2-30628-09

9. SPONSORING/MONITORING AGENCY NAME(S) AND ADDRESS(ES)
National Renewable Energy Laboratory
1617 Cole Blvd.
Golden, CO 80401-3393

10. SPONSOR/MONITOR'S ACRONYM(S)
NREL

11. SPONSORING/MONITORING AGENCY REPORT NUMBER
NREL/SR-520-38679

12. DISTRIBUTION AVAILABILITY STATEMENT
National Technical Information Service
U.S. Department of Commerce
5285 Port Royal Road
Springfield, VA 22161

13. SUPPLEMENTARY NOTES
NREL Technical Monitor: K. Brown

14. ABSTRACT *(Maximum **200 Words**)*
As a result of this work, Evergreen Solar, Inc., is now poised to take String Ribbon technology to new heights. In the ribbon growth area, Project Gemini—the growth of dual ribbons from a single crucible—has reached or exceeded all the manufacturing goals set for it. This project grew from an R&D concept to a production pilot phase and finally to a full production phase, all within the span of this subcontract. A major aspect of the overall effort was the introduction of controls and instrumentation as in-line diagnostic tools. In the ribbon production area, the result has been a 12% increase in yields, a 10% increase in machine uptime, and the flattest ribbon ever grown at Evergreen. In the cell area, advances in process development and robotic handling of Gemini wafers have contributed, along with the advances in crystal growth, to a yield improvement of 6%. Particularly noteworthy in the cell area was the refinement of the no-etch process whereby the as-grown ribbon surface could be controlled sufficiently to allow this process to succeed as well as it has. This process obviates any need for wet chemistry or etching between ribbon growth and diffusion.

15. SUBJECT TERMS
PV; string ribbon; yield; no-etch process; module; manufacturing; thin-film; capacity; in-line diagnostics;

16. SECURITY CLASSIFICATION OF:			17. LIMITATION OF ABSTRACT	18. NUMBER OF PAGES	19a. NAME OF RESPONSIBLE PERSON
a. REPORT	b. ABSTRACT	c. THIS PAGE			
Unclassified	Unclassified	Unclassified	UL		19b. TELEPONE NUMBER (*Include area code)*